NJC

RSC Publishing

PAPER

View Article Online
View Journal | View Issue

Synthetic bacteriochlorins with integral spiro-piperidine motifs†

Cite this: *New J. Chem.*, 2013, **37**, 1157

Kanumuri Ramesh Reddy,[a] Elisa Lubian,[a] M. Phani Pavan,[a] Han-Je Kim,*[b] Eunkyung Yang,[c] Dewey Holten*[c] and Jonathan S. Lindsey*[a]

A new molecular design incorporates a spiro-piperidine unit in each pyrroline ring of synthetic bacteriochlorins, thereby (1) replacing the previous geminal dimethyl group with a functionally equivalent motif to suppress adventitious dehydrogenation, (2) enabling tailoring of the bacteriochlorin by nitrogen derivatization, and (3) leaving the β-pyrrolic positions available for introduction of auxochromes to tune the spectral properties. Conversion of an N-protected 4-piperidone to the N-protected α,β-unsaturated ketone, Michael reaction with 4-(ethoxycarbonyl)-3-ethyl-2-(2-nitroethyl)pyrrole, and subsequent reductive cyclization provided the spiro-piperidine-1-methyldihydrodipyrrin. Treatment with SeO_2 followed by trimethyl orthoformate under acid catalysis converted the 1-methyl group to a 1-(1,1-dimethoxymethyl) motif. Self-condensation of the resulting spiro-piperidine-dihydrodipyrrin-acetal afforded the 5-methoxy- or 5-unsubstituted bacteriochlorin, each bearing two spiro-piperidine units. The spiro-piperidine units were derivatized at the nitrogens by methylation, sulfonylation, acylation, or quaternization; the latter with methyl iodide afforded two dicationic, hydrophilic bacteriochlorins. Altogether, eight spiro-piperidine-bacteriochlorins were prepared. Spectroscopic characterization was carried out in DMF (and in water for the quaternized, 5-methoxybacteriochlorin). Compared to the 5-unsubstituted analogue, the quaternized, 5-methoxybacteriochlorin has in DMF a shorter wavelength of the intense near-infrared absorption band (733 *vs.* 752 nm) and fluorescence band (739 *vs.* 760 nm), modestly greater fluorescence yield (0.15 *vs.* 0.08) and modestly longer lifetime of the lowest singlet excited state (4.7 *vs.* 3.3 ns). In general, the spiro-piperidinyl moiety does not significantly alter the rate constants or yields of the decay pathways (fluorescence, intersystem crossing, internal conversion) of the lowest singlet excited state of the bacteriochlorin. Taken together, the results describe a new molecular design for tailoring the polarity of near-infrared absorbers.

Received (in Montpellier, France) 23rd December 2012, Accepted 22nd January 2013

DOI: 10.1039/c3nj41161c

www.rsc.org/njc

Introduction

Bacteriochlorins (or tetrahydroporphyrins) are tetrapyrrole macrocycles that strongly absorb light in the near-infrared (NIR) spectral region (700–900 nm),[1] which makes this class of compounds attractive for a wide variety of photochemical studies encompassing artificial photosynthesis[2–5] and photomedicine.[6–18] Bacteriochlorophylls contain the bacteriochlorin chromophore and provide the basis for light-harvesting and electron-transfer processes in bacterial photosynthesis[19] (Chart 1). The synthesis of bacteriochlorins is an area of active interest.[20–26] Our own work on this topic has been devoted to the development of a *de novo* route to synthetic bacteriochlorins. The resulting bacteriochlorins contain a geminal dimethyl group in each pyrroline ring (Chart 1), thereby blocking oxidative pathways leading to unsaturated analogues (chlorins, porphyrins).[27–31]

To fulfill the rich potential of bacteriochlorins requires the availability of versatile molecular building blocks[31] that contain the bacteriochlorin chromophore thereby enabling elaboration in diverse ways. The creation of multipigment light-harvesting arrays,[32,33] for example, relies on molecular building blocks with suitably positioned synthetic handles. In this regard, few artificial photosynthetic constructs with NIR absorption have been prepared,[4,5] a lacuna attributable to the relative dearth of suitable bacteriochlorin building blocks. An attractive design is

[a] *Department of Chemistry, North Carolina State University, Raleigh, North Carolina 27695-8204, USA. E-mail: jlindsey@ncsu.edu*
[b] *Department of Science Education, Gongju National University of Education, Gongju 314-711, Korea. E-mail: hjkim@gjue.ac.kr*
[c] *Department of Chemistry, Washington University, St. Louis, Missouri 63130-4889, USA. E-mail: holten@wustl.edu*

† Electronic supplementary information (ESI) available: Spectroscopic data for new compounds. See DOI: 10.1039/c3nj41161c

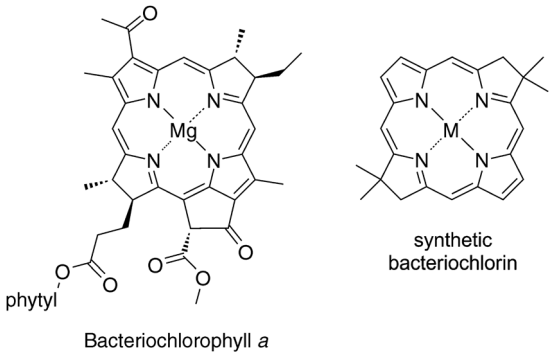

Chart 1 Naturally occurring bacteriochlorophyll *a* and a synthetic bacteriochlorin.

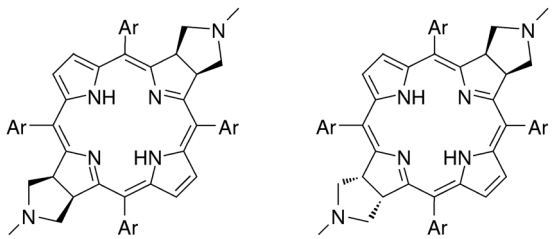

Chart 2 Diaminobacteriochlorins.

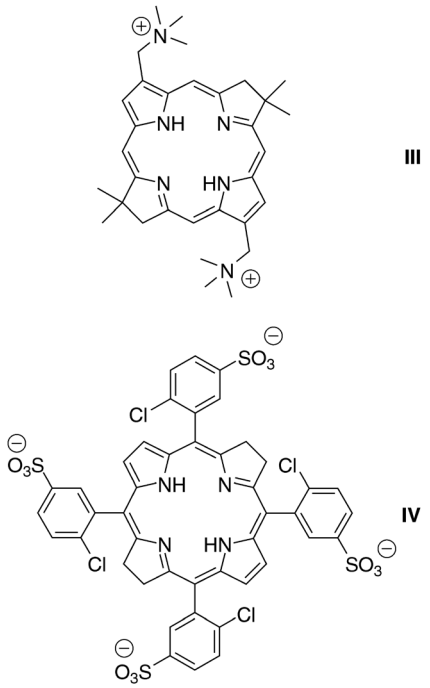

Chart 3 Representative hydrophilic, synthetic tetrapyrrole macrocycles.

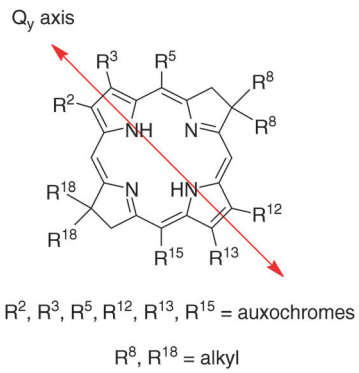

Chart 4 Design consideration for bacteriochlorins.

represented by the annulated *cis*- and *trans*-diaminobacteriochlorins of Cavaleiro *et al.*[20] (**I**, **II**, Chart 2), an architecture that has been elaborated at the *meso*-aryl sites by Drain and coworkers for studies in photomedicine.[14]

Part and parcel of the design of synthetically malleable bacteriochlorin constituents is the ability to tune the polarity from hydrophobic through amphiphilic to hydrophilic. Tetrapyrrole macrocycles are inherently hydrophobic given the neutral 18π-electron system that spans the disk-shaped hydrocarbon skeleton. Approaches for rendering tetrapyrrolic macrocycles (porphyrins, chlorins, and bacteriochlorins) more hydrophilic have included the incorporation of substituents ranging from moderate polarity (such as hydroxyalkyl or hydroxyaryl moieties) to highly polar by virtue of the presence of strongly ionizable or permanently charged groups. Examples of highly polar motifs are shown in Chart 3 and include the following: (i) a quaternized aliphatic amine for bacteriochlorins (**III**);[34] and (ii) haloarenesulfonic acids attached to the *meso* positions of synthetic bacteriochlorins (**IV**).[16] The latter design draws on two generations of chemistry concerning synthetic porphyrins that bear phenylsulfonic acid units at the *meso*-positions.[35]

Our prior studies in bacteriochlorin chemistry have revealed that the long-wavelength absorption band can be tuned across a portion of the NIR spectral region (700–820 nm) by introduction of auxochromes at the β-pyrrolic (2, 3, 12, 13) and *meso* (5, 15) positions (the 10 and 20-positions have heretofore not been accessed synthetically).[28–30,36,37] The transition that underpins the long-wavelength absorption band (Q_y) is polarized along the long axis of the molecule that bisects the respective β-pyrrolic positions[1,19,28] (Chart 4). We previously introduced a variety of substituents at the β-pyrrolic sites to tailor polarity from hydrophobic to amphiphilic to hydrophilic.[34,38] Preserving access to those positions for wavelength tunability is essential in many designs for photochemical studies. Accordingly, we considered introducing motifs in the pyrroline ring where the geminal dimethyl groups otherwise reside. Thus, the key features in the design explored herein are as follows: (i) the 8- and 18-positions – which are apart from the bacteriochlorin π-system – are employed for tailoring polarity; and (ii) the β- and *meso*- (2, 3, 5, 12, 13, and 15) positions are open for introduction of auxochromes.

A previous design of synthetic chlorins – but not bacteriochlorins – incorporated a spiro-fused cyclohexane unit at the pyrroline ring (**V**, Chart 5) in lieu of a geminal dimethyl group.[39] We sought to build on this design and incorporate functionality suitable for derivatization in the spiro-fused cyclohexane unit.

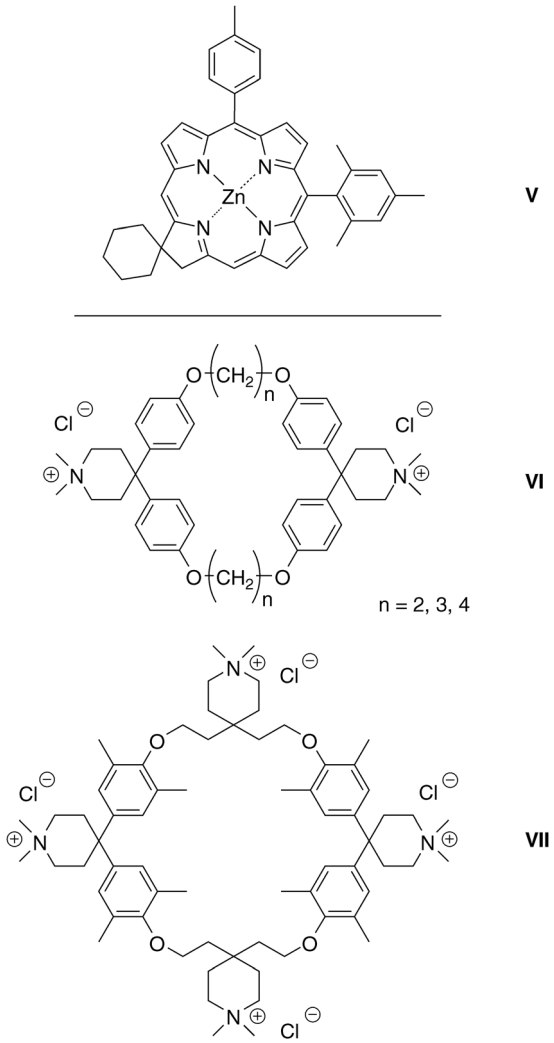

Chart 5 Prior spirohexylchlorin (top); Diederich designs for supramolecular hosts (bottom).

In this regard, we were drawn to the spiro-fused piperidine motifs (typically in the quaternized 4,4-dialkyl piperidinium form) employed by Diederich and coworkers in the designs of cyclophanes for host–guest complexation studies in water (**VI**, **VII**, Chart 5).[40–46]

In this paper, we describe the synthesis of eight bacteriochlorins wherein a spiro-piperidine unit is integrated in each pyrroline ring in lieu of the previously employed geminal dimethyl group. The spiro carbon atoms[47] are thus located at the 8 and 18-positions of the bacteriochlorin. Three key steps were extensively studied: (i) the Michael addition of an *N*-piperidinyl protected α,β-unsaturated ketone and a 2-(2-nitroethyl)pyrrole, (ii) the subsequent reductive cyclization to give the spiro-piperidine-dihydrodipyrrin, and (iii) the selenium dioxide oxidation followed by acetal formation, which provides the desired dihydrodipyrrin-acetal precursor to the bacteriochlorin. Two parent bacteriochlorins were derivatized (methylation, quaternization, acetylation, sulfonylation) at the nitrogens of the spiro-piperidine unit. Spectroscopic characterization of two dicationic bacteriochlorins was carried out in polar solvents (aqueous solution, DMF).

Results and discussion

I. Synthesis

A. Retrosynthesis. Two representative target bacteriochlorins of the present study are shown in Scheme 1. Retrosynthetic analysis shows two major transformations: (i) bacteriochlorin formation from the dihydrodipyrrin-acetal that contains a piperidine moiety integrated *via* a spiro architecture, and (ii) formation of the dihydrodipyrrin-acetal from a 2-(2-nitroethyl)-pyrrole (**2**) and a piperidine unit (**1-R**) containing the constituents to create the pyrroline ring. Thus, the bacteriochlorin β-pyrrole substituents are introduced at a very early stage of the synthesis, whereas quaternization (or other derivatization) occurs in the last step of the synthesis. The β-pyrrole substituents chosen here are identical with those in analogous bacteriochlorins studied previously.[29,37,48]

B. Initial exploration

*1. Piperidine unit **1-Me**.* The synthesis of piperidine building block **1-Me** was attempted *via* the route shown in Scheme 2. Thus, bromination of 1,1-dimethoxyacetone provided the known bromodimethoxypyruvaldehyde **3**,[49] which upon treatment with diethyl phosphite gave diethyl-1,1-dimethoxy-2-oxopropylphosphonate (**3A**). The Horner–Wadsworth–Emmons reaction of **3A** and *N*-methyl-4-piperidone (**4-Me**) under various conditions did not provide the expected product **1-Me**, but rather led to the decomposition of the phosphonate. An alternative approach entailed conversion of **3** to the Wittig reagent[50] **3B**. The reaction of the latter and **4-Me** also did not provide

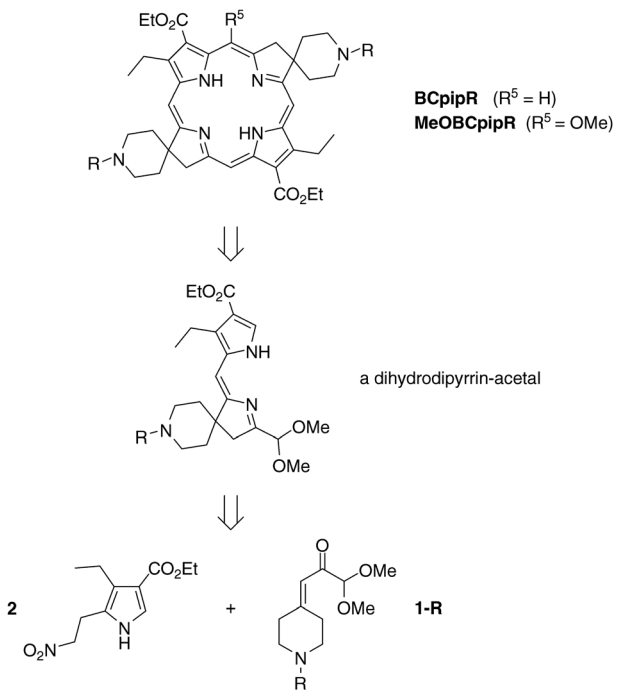

Scheme 1 Retrosynthesis of spiro-piperidine integrated bacteriochlorins.

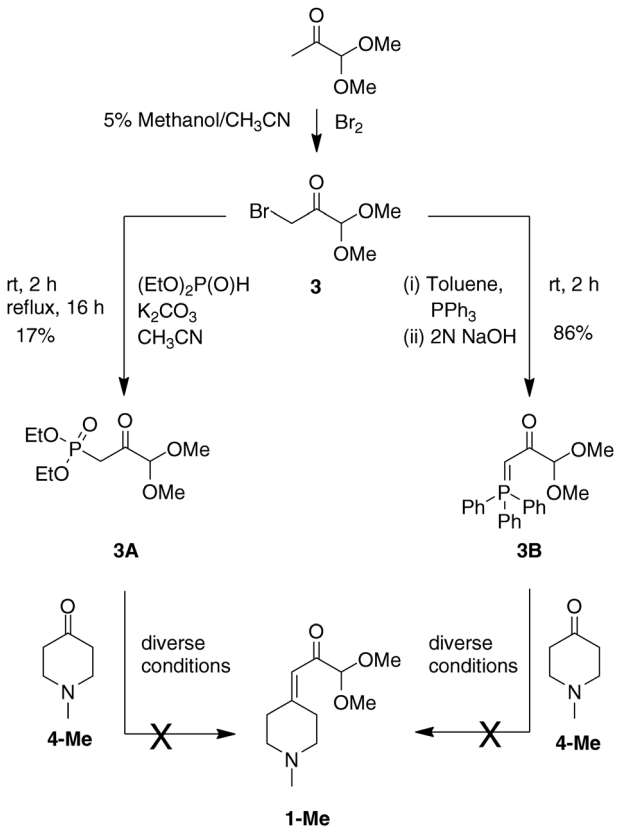

Scheme 2 Attempted synthesis of piperidine building block.

1-Me, but rather gave no reaction or decomposition of Wittig reagent **3B** (Scheme 2).

2. Dihydrodipyrrin-carboxaldehyde approach. Due to the inability to prepare *N*-methyl piperidine-acetal **1-Me** and thereby incorporate all requisite functionality in one unit, we turned to a strategy inspired by the elegant work of Jacobi *et al.*,[51] who converted a 1-methyldihydrodipyrrin to the corresponding dihydrodipyrrin-1-carboxaldehyde. As a prelude to the use of the spirohexyl-dihydrodipyrrin, we examined a gem-dimethyl substituted dihydrodipyrrin for reaction development. Thus, Michael reaction of 2-(2-nitroethyl)pyrrole **2** (ref. 29) and mesityl oxide gave the corresponding nitrohexanone-pyrrole **5**, which upon McMurry-type reductive cyclization (NaOMe and a buffered solution of $TiCl_3$ at room temperature) afforded the dihydrodipyrrin **6-Me**. Oxidation of **6-Me** with SeO_2 provided the aldehyde **6-CHO** at small scale upon chromatographic purification (Scheme 3). Extensive studies of the nature of the 1-substituent has revealed that the 1,1-dimethoxymethyl group provides superior reactivity in conversion to the bacteriochlorin.[31] Hence, conversion of the aldehyde to the dimethyl acetal was essential.

We sought a method compatible for conversion of the 1-methyldihydrodipyrrin to the 1,(1,1-dimethoxymethyl)-dihydrodipyrrin [*i.e.*, **6-Me** to **6-CH(OMe)$_2$**] that would not require purification of the intermediate aldehyde (**6-CHO**). Thus, treatment of the crude **6-CHO** with 0.4 M $LaCl_3$ in MeOH[52] or 10% I_2 in MeOH[53] resulted in decomposition of

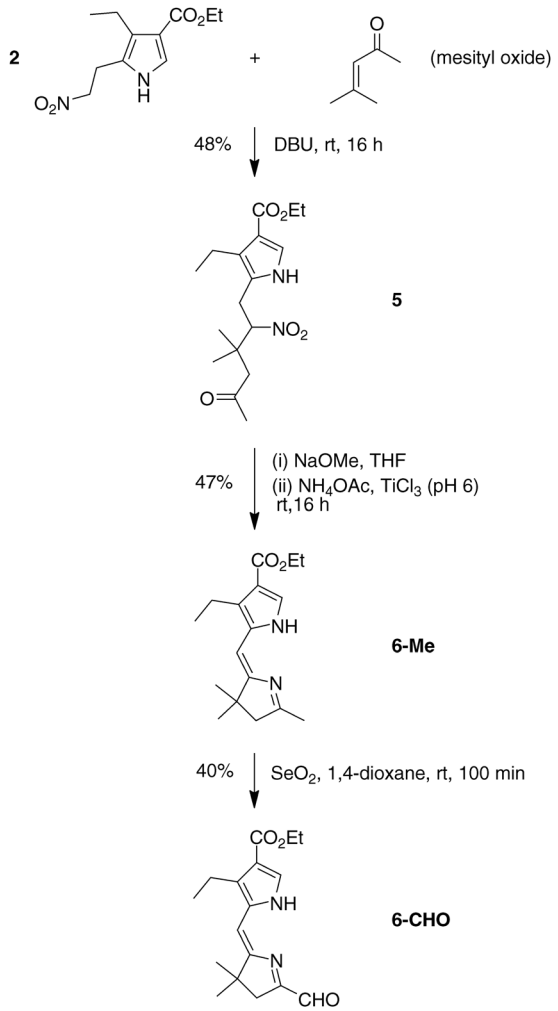

Scheme 3 Synthesis of dihydrodipyrrin-carboxaldehyde **6-CHO**.

the starting material (Table 1, entries 1 and 2). Treatment of crude **6-CHO** with 20 mol% of TsOH·H_2O and $CH(OMe)_3$ in CH_2Cl_2[54] provided the desired acetal **6-CH(OMe)$_2$**, albeit in only 20% yield (entry 3). Treatment of the crude **6-CHO** with 30 mol% TsOH·H_2O in neat $CH(OMe)_3$ provided apparently quantitative conversion to **6-CH(OMe)$_2$**; the isolated yield upon chromatography was 50% (entry 4). The data for **6-CH(OMe)$_2$** prepared in this manner were in agreement with those obtained upon Michael reaction of **2** and the α,β-unsaturated ketone–acetal 1,1-dimethoxy-4-methylpent-3-en-2-one.[29]

The absorption spectra for the dihydrodipyrrin species (**6**) are shown in Fig. 1. The aldehyde **6-CHO** absorbs in the visible region (436 nm), to be compared with the absorption at much shorter wavelength (330 nm) by the precursor **6-Me**. The clear spectral distinction between **6-Me** and **6-CHO** is invaluable because the two compounds nearly co-chromatograph, hence reliance solely on TLC analysis to gauge the progress of the reaction can be very misleading. A clean diagnostic for the progress of the conversion of **6-Me** → **6-CHO** → **6-CH(OMe)$_2$** is provided by the change in the absorption spectrum from 330 nm (**6-Me**) to 436 nm (**6-CHO**) and back to the ultraviolet region (338 nm) for **6-CH(OMe)$_2$**.

Table 1 Conversion of **6-CHO** to **6-CH(OMe)$_2$**

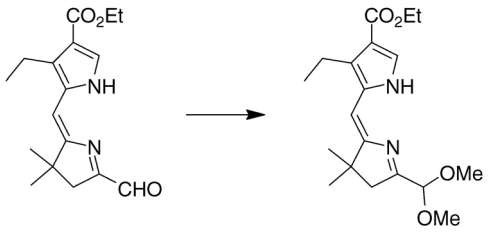

6-CHO (crude from **6-Me**) **6-CH(OMe)$_2$**

Entry	Solvent	Conditions[a]	Time (h)	Yield[b]
1	MeOH	0.4 M $LaCl_3$	3	Decomposition
2	MeOH	10% I_2	1	Decomposition
3	CH_2Cl_2	20 mol% TsOH·H_2O, $CH(OMe)_3$	3	20%
4	$CH(OMe)_3$	30 mol% TsOH·H_2O	1	50%

[a] All reactions were performed at room temperature (0.16 or 0.36 mmol scale). [b] Overall yield from **6-Me**.

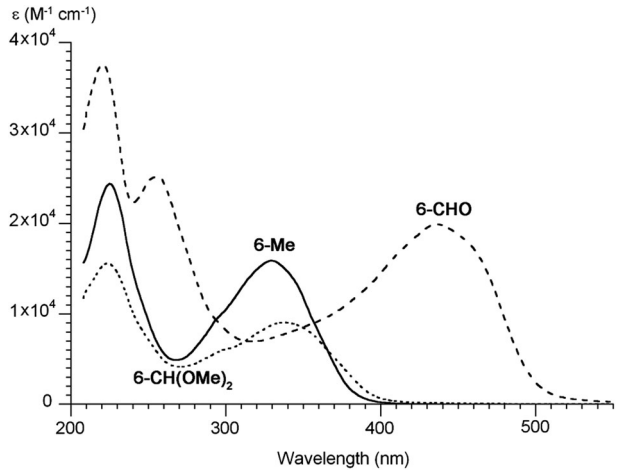

Fig. 1 Absorption spectra of dihydrodipyrrin species in diethyl ether at room temperature.

C. Synthesis of dihydrodipyrrin-acetals. The results shown in Scheme 3 and Table 1 demonstrate a new pathway to a dihydrodipyrrin-acetal using the α,β-unsaturated ketone mesityl oxide as the Michael acceptor. The Michael addition of known α,β-unsaturated ketone **7-Me**[55] and pyrrole **2** under a variety of conditions, however, afforded only the undesired isomer **7′-Me** (eqn 1).[55]

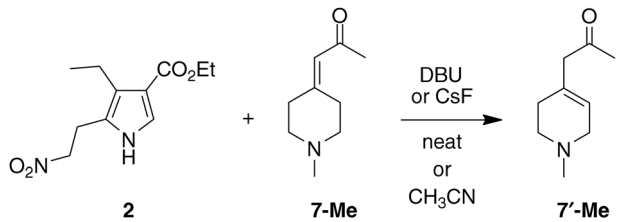

(1)

In an effort to avoid the isomerization, piperidinyl units stabilized with N-protective groups were employed as shown in Scheme 4. Accordingly, the condensation of *N*-Ts or *N*-Boc protected 4-piperidone (**4-Ts**,[56] **4-Boc**) with diethyl 2-oxopropylphosphonate[57] afforded the corresponding piperidinyl α,β-unsaturated ketone **7-Ts** or (known compound)[58] **7-Boc**. Michael reaction of each with pyrrole **2** in CH_3CN containing DBU provided the nitrohexanone **8-Ts** or **8-Boc**. (The same reaction in THF or neat did not provide good yields.) The reductive cyclization of **8-Ts** or **8-Boc** provided the spiro-N-protected-piperdine-dihydrodipyrrin (**9-Ts-Me** or **9-Boc-Me**) in

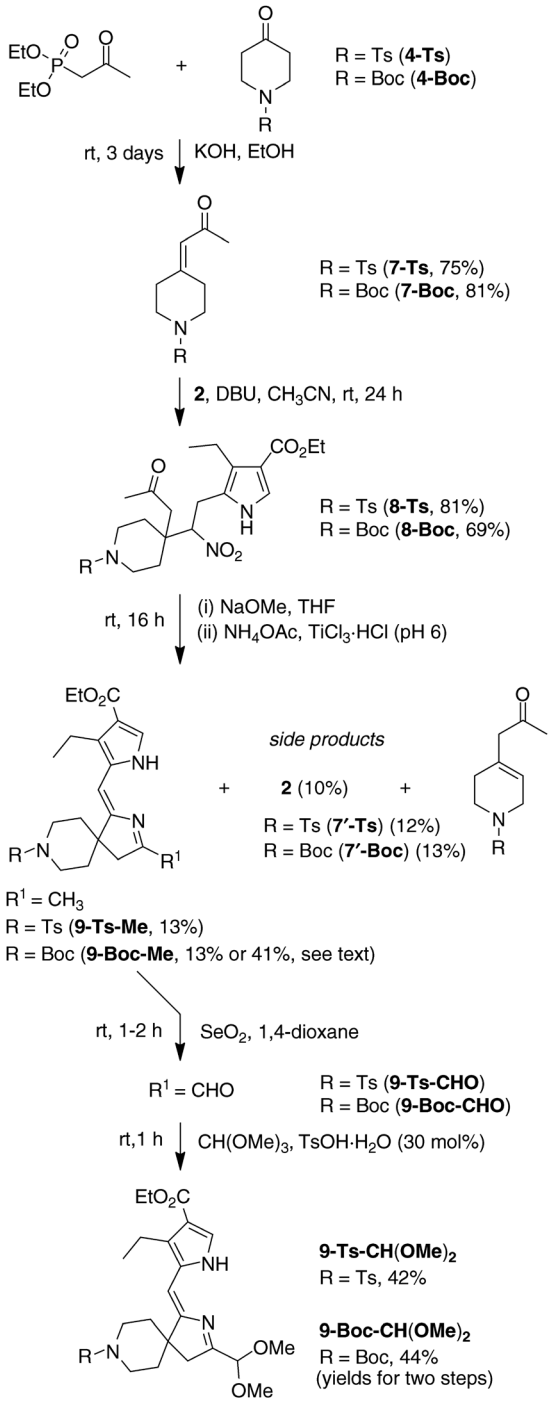

Scheme 4 Synthesis of N-protected dihydrodipyrrin-acetals.

low yield (13%). In each case we also isolated isomerized alkene **7′-Ts** (in pure form) or **7′-Boc** (not in pure form but provisionally assigned in crude form by ^{1}H NMR spectroscopy), nitroethylpyrrole **2**, and other unidentified products. The presence of **2** clearly demonstrates cleavage of the carbon–carbon bond during the reductive cyclization step, and in part accounts for the low yields of **9-Ts-Me** and **9-Boc-Me**. When the reductive cyclization of **8-Boc** was carried out for a shorter period using a lesser quantity of NaOMe, the yield of dihydrodipyrrin **9-Boc-Me** was increased from 13% to 41%. Finally, using reaction conditions similar to those described in Table 1 and Scheme 3, treatment of **9-Ts-Me** or **9-Boc-Me** with SeO_2 afforded the dihydrodipyrrin-carboxaldehyde **9-Ts-CHO** or **9-Boc-CHO**. Subsequent reaction of the crude aldehyde with trimethyl orthoformate in the presence of $TsOH{\cdot}H_2O$ (30 mol%) produced the desired **9-Ts-CH(OMe)$_2$** or **9-Boc-CH(OMe)$_2$** in 42% or 44% yield, respectively, for the two-step conversion from the 1-methyldihydrodipyrrin. Changes in the absorption spectra upon conversion of **9-Ts-Me** and **9-Boc-Me** to the corresponding **9-Ts-CH(OMe)$_2$** and **9-Boc-CH(OMe)$_2$** were nearly identical to those for **6-Me** shown in Fig. 1.

D. Synthesis of bacteriochlorins. Several distinct conditions (all at room temperature) have been developed for the self-condensation of a dihydrodipyrrin-acetal.[27,29] The conditions examined here include the following: (1) $BF_3{\cdot}OEt_2$ in CH_3CN largely affords the corresponding 5-unsubstituted bacteriochlorin;[27] and (2) TMSOTf and the proton sponge 2,6-di-*tert*-butylpyridine (2,6-DTBP) in CH_2Cl_2 affords the 5-methoxybacteriochlorin.[29] Thus, self-condensation of **9-Ts-CH(OMe)$_2$** in the presence of TMSOTf/2,6-DTBP provided the 5-methoxybacteriochlorin **MeOBCpipTs** in only 7% isolated yield (Scheme 5). Two additional bands were observed, which upon MALDI-MS analysis gave data consistent with the mono-hydroxy and dihydroxy derivatives of **MeOBCpipTs**; such bands are provisionally assigned to hydroxylation at the 7- and/or 17-position (*i.e.*, the benzylic-like methylene unit of the pyrroline ring). Oxidation of the pyrroline ring is precedented in chlorin chemistry.[39] We next turned to examine the *N*-Boc system.

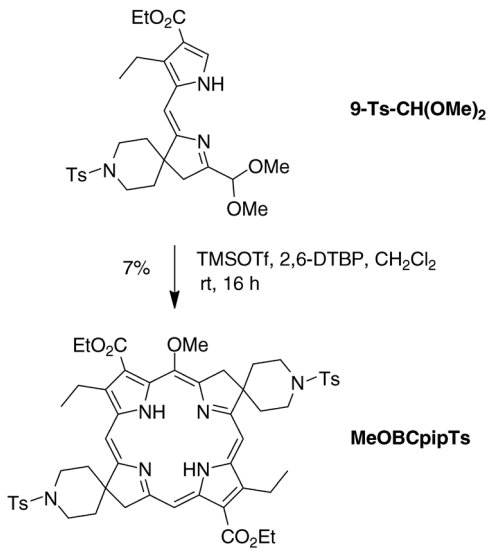

Scheme 5 Synthesis of a Ts-protected spiro-piperidine-bacteriochlorin.

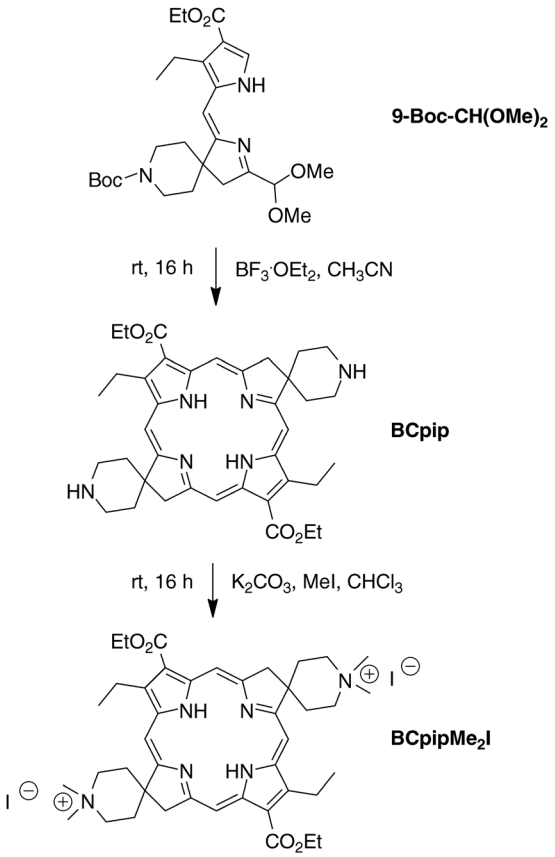

Scheme 6 Synthesis of a quaternized 5-unsubstituted bacteriochlorin.

Self-condensation of **9-Boc-CH(OMe)$_2$** in the presence of $BF_3{\cdot}OEt_2$ provided 5-unsubstituted bacteriochlorin **BCpip**. The Boc groups were cleaved under the reaction conditions, resulting in a very polar bacteriochlorin due to the presence of the two free base piperidine units. Thus, we proceeded to the quaternization step without chromatographic purification. The crude product was treated with excess of MeI in the presence of K_2CO_3 to give the bacteriochlorin target compound **BCpipMe$_2$I** (Scheme 6).

Similarly, the self-condensation of **9-Boc-CH(OMe)$_2$** in the presence of TMSOTf/2,6-DTBP[29] provided the 5-methoxybacteriochlorin **MeOBCpip** (Scheme 7). As observed for bacteriochlorin **BCpip**, the Boc groups were cleaved. The resulting bacteriochlorin also was quite polar and proved difficult to purify by chromatography. Hence, treatment of the crude reaction mixture with paraformaldehyde and $NaBH_4$ (ref. 59) provided the resulting *N*-methyl bacteriochlorin **MeOBCpipMe**, which was more readily purified by column chromatography. Treatment of **MeOBCpipMe** with excess MeI gave the hydrophilic bacteriochlorin **MeOBCpipMe$_2$I**.

Treatment of crude bacteriochlorin **MeOBCpip** with acetyl chloride or butylsulfonyl chloride gave bacteriochlorin **MeOBCpipAc** or **MeOBCpipSO$_2$Bu** in 47% or 38% yield, respectively, relative to the starting material **9-Boc-CH(OMe)$_2$** (Scheme 8). By contrast with the difficult chromatography of the parent

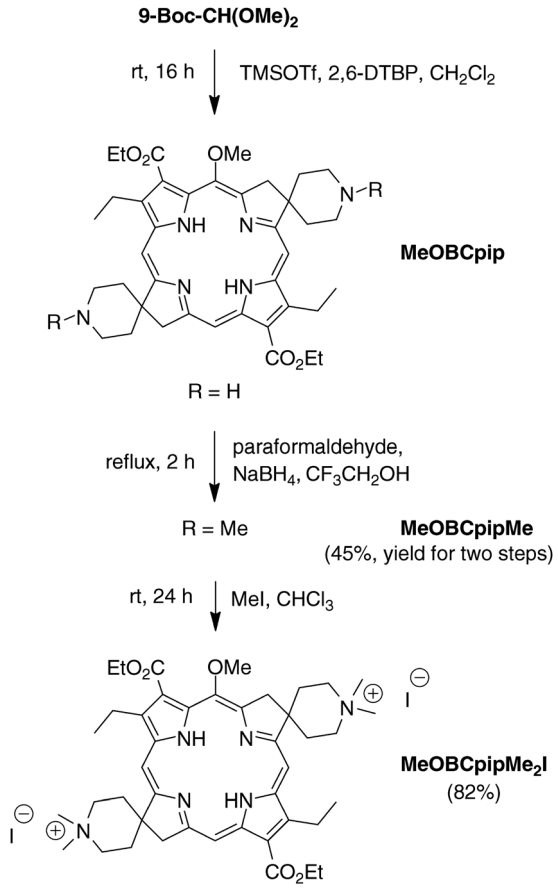

Scheme 7 Synthesis of a quaternized 5-methoxybacteriochlorin.

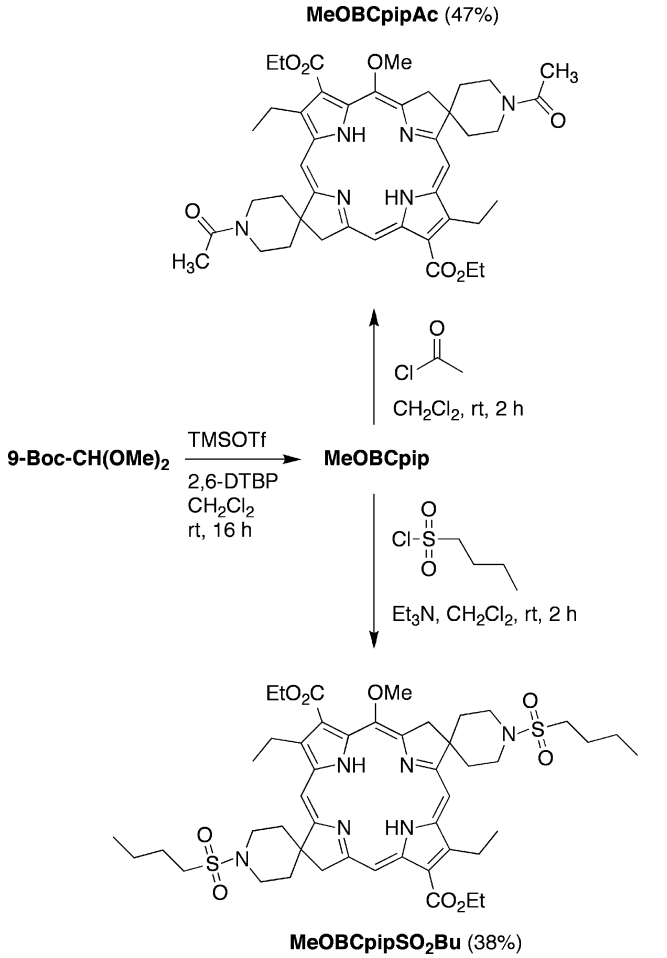

Scheme 8 Amidation of the spiro-piperidine-bacteriochlorin.

MeOBCpip, which bears two free amines, the corresponding amides were readily chromatographed on silica.

E. Chemical characterization. All precursors to the bacteriochlorins were characterized by ^{1}H NMR and ^{13}C NMR spectroscopy, and by mass spectrometry (ESI-MS). All the bacteriochlorins (except crude **BCpip** and **MeOBCpip**) were characterized by ^{1}H NMR spectroscopy, absorption spectroscopy, and mass spectrometry (ESI-MS and MALDI-MS[60]). Four of the target bacteriochlorins also were characterized by fluorescence spectroscopy (*vide infra*). Most of the new dihydrodipyrrins and precursors thereto were also characterized by ^{15}N NMR spectroscopy. The spiro-piperidine-dihydrodipyrrins each contain three distinct nitrogen atoms. For the two nitrohexanone-pyrroles (**8-Ts** and **8-Boc**) and the four dihydrodipyrrins (**9** series), a single N–H unit is present; in each case proton coupled HSQC (heteronuclear single quantum coherence) analysis gave a single peak (Table 2). Heteronuclear multiple bond correlation (HMBC) of each dihydrodipyrrin examined (**9-Ts-Me**, **9-Boc-Me**, **9-Boc-CH(OMe)$_2$**) showed three peaks corresponding to the distinct environment of the pyrrole nitrogen, pyrroline nitrogen, and N-protected (Ts or Boc) piperidine nitrogen (Table 2).

Table 2 ^{15}N NMR spectroscopic data[a]

	δ ^{15}N NMR resonance[b] (ppm)			
Compound	HSQC	HMBC		
8-Ts	−224.5	[c]		
8-Boc	−224.4	[c]		
9-Ts-Me	−228.6	−228.6	−77.8	0.2
9-Boc-Me	−228.6	−228.4	−77.1	0.2
9-Ts-CH(OMe)$_2$	−229.0	[c]		
9-Boc-CH(OMe)$_2$	−229.0	−228.4	−78.0	0.1

[a] Data were collected over the concentration range of 0.16–0.19 M samples in DMSO-d_6 at room temperature. [b] Chemical shifts were standardized with the ^{15}N-pyrrole chemical shift (δ −230.1 ppm) as an indirect reference. [c] Data not collected.

II. Photophysical characterization

A. Absorption and fluorescence spectra. The photophysical properties of four spiro-piperidine-bacteriochlorins **MeOBCpipMe$_2$I**, **BCpipMe$_2$I**, **MeOBCpipAc**, and **MeOBCpipSO$_2$Bu** were investigated in DMF. Studies were also performed for **MeOBCpipMe$_2$I** in deionized water. **BCpipMe$_2$I** was not sufficiently soluble in water to obtain trustworthy photophysical information. Similarly, **MeOBCpipMe$_2$I** or **BCpipMe$_2$I** did not give observable peaks upon ^{1}H NMR and ^{13}C NMR spectroscopy in D_2O owing to slight or negligible solubility, respectively, in aqueous media. Photophysical studies were also performed on reference bacteriochlorins **BCEtEs** and **MeOBCEtEs** (Chart 6) prepared previously.[29]

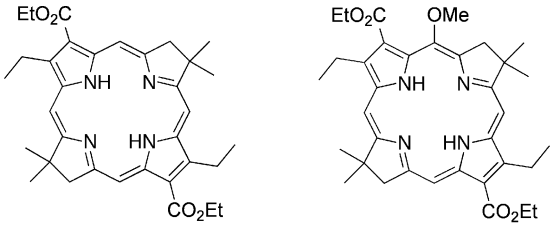

Chart 6 Benchmark bacteriochlorins.

The reference compounds contain ethyl and ethoxycarbonyl substituents at the 2,12- and 3,13- sites, respectively, a geminal dimethyl group in each pyrroline ring, and –H or $–OCH_3$ at the 5-position. The photophysical characteristics of **BCEtEs** and **MeOBCEtEs** in toluene have been studied previously.[48] The data were acquired again here for the two reference bacteriochlorins in DMF to allow the closest comparison with the results for the four spiro-piperidine-bacteriochlorins in the same medium.

Absorption and fluorescence spectra for compounds are shown in Fig. 2. Each compound exhibits a typical bacteriochlorin absorption spectrum.[1] Progressing from shorter to longer wavelengths, the spectra contain a strong $B_y(0,0)$ band (~350 nm) and $B_x(0,0)$ band (~380 nm) of comparable or slightly lower strength in the near UV region; these features are also known as the Soret bands. A weaker $Q_x(0,0)$ band (~520 nm) is observed in the visible region. The strong feature in the NIR region is the $Q_y(0,0)$ band (730–760 nm). The latter feature corresponds to excitation from the ground state to the lowest singlet excited state.

The peak positions of the four major features, the full-width-at-half maximum (FWHM) of the $Q_y(0,0)$ band, and the peak-intensity ratio of the $Q_y(0,0)$ band to the Soret (B) maximum are collected in Table 3. Fig. 2 also shows the fluorescence spectrum of each bacteriochlorin. The emission is dominated by the $Q_y(0,0)$ fluorescence band, which lies on the average 6 nm to longer wavelength and has a FWHM on the average 2 nm greater than the $Q_y(0,0)$ absorption feature (Table 3).

Reference bacteriochlorin **BCEtEs** in DMF and toluene and reference bacteriochlorin **MeOBCEtEs** in toluene show a sharp $Q_y(0,0)$ absorption band (FWHM 18–19 nm), a sharp $Q_y(0,0)$ fluorescence band (20–21 nm), and a near-unity Q_y/B absorption peak-intensity ratio (0.95–1.1). The same is true for the two spiro-piperidine-bacteriochlorins **MeOBCpipAc** and **MeOBCpipSO$_2$Bu** that lack the quaternized, positively charged nitrogen (and iodide counterion).

In contrast, the $Q_y(0,0)$ absorption band of the quaternized counterparts **MeOBCpipMe$_2$I** and **BCpipMe$_2$I** in DMF is slightly broader (20–21 nm) and even more so for the $Q_y(0,0)$ fluorescence band (23–27 nm). This broadening may result in part from a contribution of aggregation. Perhaps the clearest evidence of this effect is a slight increase in the underlying baseline as the absorption spectrum progresses into the near-UV region, which may contribute to the decrease in the Q_y/B peak intensity ratio (0.64–0.85) for **MeOBCpipMe$_2$I** and **BCpipMe$_2$I** (Table 3). Roughly the same effects are observed for

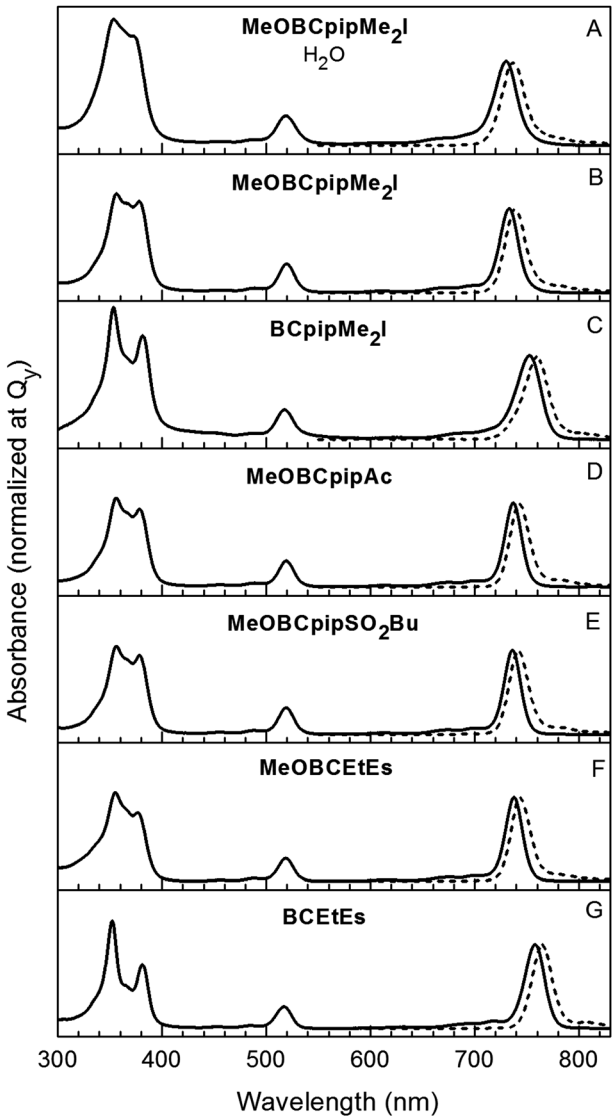

Fig. 2 Absorption spectra (solid) and fluorescence spectra (dashed) of bacteriochlorins at room temperature. The compounds were in DMF solution in all cases except for **MeOBCpipMe$_2$I** in deionized water in Panel (A). Spectral parameters are given in Table 3.

benchmark bacteriochlorin **MeOBCEtEs** in DMF (*versus* toluene). The most substantial $Q_y(0,0)$ spectral broadening (26 nm FWHM in absorption and emission) and a significant reduction in the Q_y/B absorption peak intensity ratio (0.67) occurs for quaternized spiro-piperidine-bacteriochlorin **MeOBCpipMe$_2$I** in water. Again, these effects likely represent aggregation due to limited solubility in water. As noted above, the companion quaternized compound **BCpipMe$_2$I** is even less soluble in water and reliable photophysical data could not be obtained.

Inspection of Fig. 2 and Table 3 also reveals that the spiro-piperidine-bacteriochlorins show the hypsochromic effect of a 5-methoxy group on the $Q_y(0,0)$ absorption band that has been observed for other synthetic bacteriochlorins.[29,48] In particular, comparing compounds in DMF, the $Q_y(0,0)$ band for **MeOBCpipMe$_2$I** (733 nm) lies 29 nm to shorter wavelength than

Table 3 Spectral properties of bacteriochlorins[a]

Compound	Solvent	B_y abs (nm)	B_x abs (nm)	Q_x abs (nm)	Q_y abs (nm)	Q_y abs FWHM (nm)	$\frac{I_{Q_y}}{B_{max}}$	Q_y em (nm)	Q_y em FWHM (nm)
MeOBCpipMe$_2$I	H_2O	353	372	519	730	26	0.67	736	26
	DMF	357	378	520	733	21	0.85	739	23
BCpipMe$_2$I	DMF	354	382	518	752	20	0.64	760	27
MeOBCpipAc	DMF	356	379	519	737	19	0.95	743	22
MeOBCpipSO$_2$Bu	DMF	356	378	519	736	19	0.96	742	22
MeOBCEtEs	DMF	355	376	518	738	23	0.79	745	22
	Toluene[b]	357	379	521	739	18	1.10	741	21
BCEtEs	DMF	352	381	517	759	19	0.95	765	20
	Toluene[b]	354	384	520	760	19	0.98	764	20

[a] Data acquired at room temperature. [b] Data for **MeOBCEtEs** and **BCEtEs** in toluene is from ref. 48.

Table 4 Photophysical properties of bacteriochlorins[a]

Compound	Solvent	τ_s (ns)	Φ_f B/Q_x exc	Φ_{isc}	Φ_{ic}	$(k_f)^{-1}$ (ns)	$(k_{isc})^{-1}$ (ns)	$(k_{ic})^{-1}$ (ns)
MeOBCpipMe$_2$I	H_2O	3.4	0.09	0.34	0.57	38	10	6
	DMF	4.7	0.15	0.39	0.46	31	12	10
BCpipMe$_2$I	DMF	3.3	0.08	0.35	0.57	41	9	6
MeOBCpipAc	DMF	4.8	0.18	0.37	0.45	27	13	11
MeOBCpipSO$_2$Bu	DMF	4.7	0.18	0.38	0.44	26	12	11
MeOBCEtEs	DMF	4.2	0.17	0.47	0.36	25	9	12
	Toluene[b]	4.3	0.17	0.63	0.20	25	7	22
BCEtEs	DMF	3.3	0.12	0.35	0.53	28	9	6
	Toluene[b]	3.3	0.14	0.55	0.31	24	6	11

[a] Data acquired at room temperature in Ar-purged solutions. [b] Data for **MeOBCEtEs** and **BCEtEs**.

that for **BCpipMe$_2$I** (752 nm). This effect parallels the 21 nm hypsochromic shift in Q_y(0,0) position for benchmark **MeOBCEtEs** (738 nm) *versus* **BCEtEs** (759 nm). Furthermore, comparison of the Q_y(0,0) absorption positions of **MeOBCpipMe$_2$I** (733 nm) *versus* **MeOBCpipAc** (737 nm) and **MeOBCpipSO$_2$Bu** (736 nm) reveals a modest (3–4 nm) effect of quaternization of the nitrogen in the spiro-piperidine moiety.

B. Fluorescence quantum yields and excited-state lifetimes. The fluorescence quantum yields (Φ_f) of the spiro-piperidine-bacteriochlorins and reference compounds are listed in Table 4. These yields were determined for each compound using excitation in the Soret region (~385 nm) and the Q_x region (~520 nm) and the average value is reported. The Φ_f and τ_s values (0.15, 4.7 ns) for **MeOBCpipMe$_2$I** in DMF are both reduced from those (0.08, 3.3 ns) for analogue **BCpipMe$_2$I** that lacks the 5-methoxy group. The values (in DMF) for analogues **MeOBCpipAc** (0.18, 4.8 ns) and **MeOBCpipSO$_2$Bu** (0.18, 4.7 ns) that also bear the 5-methoxy group but do not have the quaternized nitrogen in the piperidine ring are similar to one another and to those for **MeOBCpipMe$_2$I**. The reduced Φ_f and τ_s values for **MeOBCpipMe$_2$I** *versus* **BCpipMe$_2$I** parallel a number of other findings, including (1) those obtained here in DMF for benchmark **MeOBCEtEs** (0.17, 4.2 ns) *versus* **BCEtEs** (0.12, 3.3 ns), (2) those obtained previously[48] in toluene for the same pair of compounds (0.17, 4.3 ns) *versus* (0.14, 3.3 ns), and (3) those obtained for other pairs of synthetic bacteriochlorins with or without a 5-methoxy substituent.

Inspection of Table 4 also shows that the Φ_f and τ_s values for **MeOBCpipMe$_2$I** in water (0.09, 3.4 ns) are reduced by about 30% for the compound in DMF (0.15, 4.7 ns). Nonetheless, the long singlet excited-state lifetime and modest fluorescence yield of **MeOBCpipMe$_2$I** in both water and DMF, and similarly for **BCpipMe$_2$I**, **MeOBCpipAc** and **MeOBCpipSO$_2$Bu** in DMF indicate that incorporation of the spiro-piperidine motif does not compromise the photophysical properties of the bacteriochlorin, which are essentially identical with those of bacteriochlorins bearing a geminal dimethyl motif in each pyrroline ring.

C. Triplet and internal conversion quantum yields and rate constants for the singlet excited-state decay pathways. Table 4 gives the measured yield of intersystem crossing (Φ_{isc}) from the lowest singlet to triplet excited state (*e.g.*, the triplet yield) for each bacteriochlorin. The values for the four spiro-piperidine-bacteriochlorins are in the range 0.34–0.39, which are slightly lower than those for the benchmarks (0.35–0.63) in DMF and toluene (Table 4) and the average value of 0.52 obtained previously for a large set of synthetic free base bacteriochlorins.[48]

The quantum yield of the third decay pathway of the lowest singlet excited state, nonradiative internal conversion to the ground state, can be calculated by difference using the expression $\Phi_{ic} = 1 - \Phi_f - \Phi_{isc}$. The Φ_{ic} values are reported in Table 4 and are in the range 0.44–0.57 for the four spiro-piperidine-bacteriochlorins and 0.20–0.53 for the benchmarks.

The rate constants for the three excited-state decay processes can be obtained from the singlet excited-state lifetime (τ_s) and the respective yield using the formula $k_i = \Phi_i/\tau_s$, where i = f, isc, and ic for fluorescence, intersystem crossing and internal conversion, respectively. The resulting values are given in Table 4 as the inverse of the k_i values (in units of nanoseconds). Incorporation of the spiro-piperidine moiety may slightly

decrease the radiative rate constant (k_f), slightly decrease the intersystem-crossing rate constant (k_{isc}) and slightly increase the internal conversion rate constant (k_{ic}) with corresponding small to modest effects on the respective yields Φ_f, Φ_{isc} and Φ_{ic}. These trends are true even for **MeOBCpipMe$_2$I** dissolved in water *versus* DMF. Thus, the spiro-piperidine motif does not have a significant effect on the fundamental electronic properties (the rate constants) that underlie the photophysical characteristics and excited-state processes of the bacteriochlorin macrocycle.

Outlook

Synthetic bacteriochlorins are invaluable for studies in artificial photosynthesis and in photomedicine given their strong absorption in the NIR spectral region. Nonetheless, the synthetic methodology for the preparation of bacteriochlorin building blocks[26] is in an embryonic state relative to that of porphyrins.[61,62] The synthesis of *N*-Boc protected dihydrodipyrrin-acetal **9-Boc-CH(OMe)$_2$** provides a convenient intermediate on the path to bacteriochlorins that bear a piperidine motif integrated *via* spiro-fusion in each pyrroline ring. The nitrogen of the piperidine motif is conveniently derivatized by mono- or dimethylation, acetylation, or sulfonylation, and in principle, by a wide variety of other procedures.[63,64] To our knowledge, the closest analogues of diamino-bacteriochlorins **BCpip** and **MeOBCpip** appear to be the annulated *cis*- and *trans*-diaminobacteriochlorins **I** and **II** (Chart 2).[14,20] In both types of architectures (**BCpipMe$_2$I**, **MeOBCpipMe$_2$I**; **I**, **II**) the amino groups are embedded in rings that are integral to the pyrrolines of the bacteriochlorin, thereby leaving the *meso*- and β-pyrrolic sites of the macrocycle open for other types of substituents.

The availability of open β-pyrrole sites despite introduction of the spiro-piperidine motif is a valuable design feature for photochemical studies. The β-pyrrole positions lie along the axis of the bacteriochlorin that is coincident with the polarization of the Q_y transition,[1,19,28] and hence are the most sensitive to the introduction of auxochromes for tuning spectral properties. The long singlet excited-state lifetime and modest fluorescence yield of **MeOBCpipMe$_2$I** in both water and DMF, and similarly for **BCpipMe$_2$I**, **MeOBCpipAc** and **MeOBCpipSO$_2$Bu** in DMF indicate that incorporation of the spiro-piperidine motif does not compromise photophysical properties of the bacteriochlorin. Accordingly, the spiro-piperidine-bacteriochlorins are synthetically malleable candidates for use in a wide variety of studies in artificial photosynthesis, solar energy and photomedicine.

Experimental section

General methods

^{1}H NMR (300 MHz), ^{13}C NMR (100 MHz), ^{15}N NMR (41 MHz) or ^{31}P NMR (162 MHz) spectroscopy was performed at room temperature in $CDCl_3$ unless noted otherwise. All ^{15}N NMR spectra were collected with samples at concentrations of 0.16–0.19 M in DMSO-d_6 at room temperature. The chemical shifts are reported with the resonance of ^{15}N pyrrole (δ −230.1 ppm) as an indirect reference. All ^{31}P chemical shifts are reported *versus* the resonance of H_3PO_4 as an external reference (insert tube). Silica gel (40 μm average particle size) was used for column chromatography. All solvents were reagent grade and were used as received unless noted otherwise. THF was freshly distilled from sodium/benzophenone ketyl. Matrix-assisted laser-desorption mass spectrometry (MALDI-MS) was performed with the matrix 1,4-bis(5-phenyl-2-oxaxol-2-yl)benzene (POPOP).[60] Electrospray ionization mass spectrometry (ESI-MS) data are reported for the molecular ion, protonated molecular ion, or sodium-cationized molecular ion. The known compounds **2**,[29] **3**,[49] **4-Ts**,[56] and **7-Me**[55] were prepared according to literature procedures. The spiro nomenclature is given according to the literature.[47]

Diethyl 3,3-dimethoxy-2-oxopropylphosphonate (3A)

A solution of 3-bromo-1,1-dimethoxypropan-2-one (**3**, 5.00 g, 25.4 mmol) in acetonitrile (50 mL) was treated with K_2CO_3 (4.38 g, 31.7 mmol) and stirred at room temperature for 2 h. Diethyl phosphite was added, and the reaction mixture was heated under reflux. After 16 h, acetonitrile was evaporated under reduced pressure, and water was added. The mixture was extracted with diethyl ether. The organic layer was washed with water, dried (Na_2SO_4), and concentrated. Column chromatography [silica, ethyl acetate–hexanes (3 : 2)] afforded a colorless oil (0.98 g, 17%): ^{1}H NMR δ 1.31–1.38 (m, 6H), 2.99–3.09 (m, 2H), 3.45 (s, 3H), 3.46 (s, 3H), 4.14–4.24 (m, 4H), 4.75 (d, J = 2.4 Hz, 1H); ^{13}C NMR δ 16.6 (d, J = 5.3 Hz), 46.9, 54.3 (d, J = 197.2 Hz), 55.9 (d, J = 67.4 Hz), 63.3 (d, J = 6.8 Hz), 63.6 (d, J = 6.8 Hz), 101.4 (d, J = 21.2 Hz) (the carbonyl carbon was not observed); ^{31}P NMR δ 18.4; ESI-MS obsd 277.0812, calcd 277.0811 [$(M + H)^+$, M = $C_9H_{19}O_6P$].

3,3-Dimethoxy-2-oxopropyl-1-(triphenylphosphoranylidene) (3B)

A solution of PPh_3 (12.9 g, 49.2 mmol) in dry toluene (25 mL) was treated dropwise with **3** (9.60 g, 49.2 mmol) in toluene (10 mL) at room temperature. After 2 h, the white precipitate (phosphonium bromide salt) was filtered and washed with cold toluene (20 mL) and hexanes (20 mL). The filtrate was discarded. Water was added to dissolve the phosphonium bromide salt. The resulting solution was extracted with diethyl ether to remove further organic impurities. The aqueous solution was cooled in an ice bath, whereupon 2 N aqueous NaOH was added slowly until pH 8–10 was obtained. The crystalline phosphorane was collected by filtration, washed thoroughly with cold water, and dried under vacuum (16.0 g, 86%): mp 120–122 °C; ^{1}H NMR (400 MHz) δ 3.45 (s, 6H), 4.22 (d, J = 24.0 Hz, 1H), 4.63 (s, 1H), 7.42–7.49 (m, 6H), 7.52–7.59 (m, 3H), 7.62–7.71 (m, 6H); ^{13}C NMR δ 50.8 (d, J = 427.6 Hz), 54.0, 104.6 (d, J = 60.8 Hz), 126.7 (d, J = 360.8 Hz), 129.0 (d, J = 48.4 Hz), 132.3 (d, J = 9.2 Hz), 133.3 (d, J = 42.8 Hz), 186.7; ^{31}P NMR δ 17.3; ESI-MS obsd 379.1455, calcd 379.1458 [$(M + H)^+$, M = $C_{23}H_{23}O_3P$].

6-(4-Ethoxycarbonyl-3-ethylpyrrol-2-yl)-4,4-dimethyl-5-nitrohexa-2-one (5)

Following a standard method,[52] a solution of **2** (3.81 g, 15.9 mmol) and mesityl oxide (5.44 mL, 47.6 mmol) was treated with DBU (7.11 mL, 47.6 mmol). The reaction mixture was stirred for 16 h at room temperature, diluted with ethyl acetate, and washed with a saturated aqueous solution of NH_4Cl and brine. The organic layer was dried (Na_2SO_4) and concentrated. Excess mesityl oxide was removed under reduced pressure. The resulting oil was chromatographed [silica, ethyl acetate–hexanes (1 : 2)] to afford a dark brown solid (2.6 g, 48%): mp 96–98 °C; ^{1}H NMR (400 MHz) δ 1.13 (s, 3H), 1.15 (t, J = 7.2 Hz, 3H), 1.27 (s, 3H), 1.32 (t, J = 7.2 Hz, 3H), 2.17 (s, 3H), 2.44 (d, J = 17.4 Hz, 1H), 2.62 (d, J = 17.4 Hz, 1H), 2.56–2.74 (m, 2H), 3.01 (ABX, ^3J = 2.4 Hz, ^2J = 15.4 Hz, 1H), 3.27 (ABX, ^3J = 11.6 Hz, ^2J = 15.4 Hz, 1H), 4.25 (q, J = 7.2 Hz, 2H), 5.08 (ABX, ^3J = 2.4 Hz, ^3J = 11.6 Hz, 1H), 7.26–7.27 (m, 1H), 8.23 (brs, 1H); ^{13}C NMR δ 14.6, 16.2, 18.2, 24.3, 24.5, 24.5, 32.1, 37.0, 51.7, 59.5, 94.6, 114.6, 123.3, 124.2, 125.2, 165.3, 207.4; ESI-MS obsd 361.1728, calcd 361.1734 [$(M + Na)^+$, M = $C_{17}H_{26}N_2O_5$].

8-Ethoxycarbonyl-7-ethyl-2,3-dihydro-1,3,3-trimethyldipyrrin (6-Me)

Following a standard method,[29] in a first flask, a solution of **5** (2.05 g, 6.06 mmol) in freshly distilled THF (30 mL) was treated with NaOMe (1.64 g, 30.3 mmol) under argon at 0 °C. The mixture was stirred and degassed by bubbling argon through the solution for 1 h. In a second flask, $TiCl_3$ (23.0 mL, 20 wt% in 3% HCl solution, 36.4 mmol), THF (61 mL), NH_4OAc (23.0 g, 298 mmol), and degassed deionized water (6 mL, degassed with argon for 30 min) were combined under argon and the mixture was degassed by bubbling with argon for 45 min. Then, the first flask mixture was transferred *via* cannula to the buffered $TiCl_3$ mixture. The resulting mixture was stirred at room temperature for 16 h under argon. The mixture was treated with a saturated aqueous solution of $NaHCO_3$ (120 mL), and extracted with ethyl acetate. The organic extract was washed with water, dried ($NaSO_4$), and concentrated. Column chromatography [silica, hexanes–ethyl acetate (3 : 1)] afforded a pale yellow oil (820 mg, 47%): ^{1}H NMR (400 MHz) δ 1.16 (t, J = 7.6 Hz, 3H), 1.22 (s, 6H), 1.34 (t, J = 7.2 Hz, 3H), 2.21 (s, 3H), 2.52 (s, 2H), 2.80 (q, J = 7.6 Hz, 2H), 4.27 (q, J = 7.2 Hz, 2H), 5.71 (s, 1H), 7.39–7.40 (m, 1H), 11.08–11.21 (brs, 1H); ^{13}C NMR δ 14.7, 16.5, 18.1, 20.8, 29.4, 41.4, 54.0, 59.3, 101.4, 114.1, 124.6, 125.2, 128.7, 161.4, 165.8, 177.2; ESI-MS obsd 289.1904, calcd 289.1911 [$(M + H)^+$, M = $C_{17}H_{24}N_2O_2$]; λ_{abs} (toluene) 332 nm; λ_{abs} (diethyl ether) 330 nm.

8-Ethoxycarbonyl-7-ethyl-1-formyl-2,3-dihydro-3,3-dimethyldipyrrin (6-CHO)

A solution of **6-Me** (29.0 mg, 0.10 mmol) in 1,4-dioxane (2.0 mL) was treated with SeO_2 (33.0 mg, 0.30 mmol) under argon. The mixture was stirred at room temperature, and the progress of the reaction was monitored by UV-Visible spectroscopy. After 100 min, the reaction mixture was diluted with ethyl acetate (10 mL) and treated with a saturated aqueous solution of $NaHCO_3$ (2.0 mL). The organic layer was washed with water (2 mL), dried (Na_2SO_4), and concentrated. Column chromatography [silica, ethyl acetate–hexanes (1 : 3)] afforded a yellowish orange oil (12 mg, 40%): ^{1}H NMR (400 MHz) δ 1.20 (t, J = 7.5 Hz, 3H), 1.23 (s, 6H), 1.36 (t, J = 7.2 Hz, 3H), 2.73 (s, 2H), 2.82–2.91 (q, 2H), 4.25–4.34 (q, 2H), 6.18 (s, 1H), 7.53 (d, J = 3.3 Hz, 1H), 9.98 (s, 1H), 10.81 (brs, 1H); ^{13}C NMR δ 14.7, 16.6, 18.3, 29.4, 41.2, 46.2, 59.7, 111.2, 115.1, 127.5, 128.4, 130.5, 160.8, 165.2, 169.5, 190.1; ESI-MS obsd 303.1700, calcd 303.1703 [$(M + H)^+$, M = $C_{17}H_{22}N_2O_3$]; λ_{abs} (toluene) 455 nm; λ_{abs} (diethyl ether) 436 nm.

8-Ethoxycarbonyl-7-ethyl-2,3-dihydro-1-(1,1-dimethoxymethyl)-3,3-dimethyldipyrrin (6-CH(OMe)$_2$)

A solution of **6-Me** (0.103 g, 0.357 mmol) in 1,4-dioxane (7.0 mL) was treated with SeO_2 (119 mg, 1.07 mmol) under argon. The reaction mixture was stirred at room temperature, and the progress of the reaction was monitored by UV-Visible spectroscopy. After 1 h, the reaction mixture was diluted with ethyl acetate, washed with water, dried (Na_2SO_4), and concentrated; the crude product was used in the next step without any further purification. The crude **6-CHO** was dissolved in trimethyl orthoformate (3.0 mL), and $TsOH{\cdot}H_2O$ (20.0 mg, 0.107 mmol) was added at room temperature under argon. The progress of the reaction was monitored by UV-Visible spectroscopy. After 1 h, the reaction mixture was diluted with ethyl acetate, washed with water, dried (Na_2SO_4), and concentrated. Column chromatography [silica, ethyl acetate–hexanes (3 : 1)] afforded a yellow oil (62 mg, 50%): ^{1}H NMR (400 MHz) δ 1.17 (t, J = 7.4 Hz, 3H), 1.23 (s, 6H), 1.34 (t, J = 7.2 Hz, 3H), 2.63 (s, 2H), 2.81 (q, J = 7.4 Hz, 2H), 3.45 (s, 6H), 4.27 (q, J = 7.2 Hz, 2H), 5.03 (s, 1H), 5.86 (s, 1H), 7.42 (d, J = 3.2 Hz, 1H), 10.92 (brs, 1H); ^{13}C NMR δ 14.7, 16.5, 18.2, 29.4, 40.4, 48.4, 54.8, 59.4, 102.8, 104.5, 114.3, 125.3, 126.4, 128.3, 160.2, 165.6, 174.8; ESI-MS obsd 349.2118; calcd 349.2122 [$(M + H)^+$, M = $C_{19}H_{28}N_2O_4$]; λ_{abs} (toluene) 345 nm; λ_{abs} (diethyl ether) 338 nm. The aforementioned data are in agreement with those for the same compound obtained *via* an independent route.[29]

1-(*N*-Tosylpiperidin-4-ylidene)propan-2-one (7-Ts)

A solution of diethyl 2-oxopropyl phosphonate (9.96 g, 51.3 mmol) and KOH (2.44 g, 43.5 mmol) in ethanol (60 mL) at 5 °C was treated with **4-Ts** (10.0 g, 39.5 mmol) and stirred at room temperature. After 3 days, the mixture was concentrated to dryness. The residue was triturated several times with diethyl ether at room temperature. The resulting ether solution was dried (Na_2SO_4) and concentrated. Column chromatography [silica, ethyl acetate–hexanes (2 : 3)] afforded a white solid (8.68 g, 75%): mp 60–62 °C; ^{1}H NMR δ 2.14 (s, 3H), 2.32–2.38 (m, 2H), 2.42 (s, 3H), 2.97–3.03 (m, 2H), 3.05–3.11 (m, 2H), 3.12–3.17 (m, 2H), 6.02 (s, 1H), 7.32 (d, J = 8.1 Hz, 2H), 7.63 (d, J = 8.4 Hz, 2H); ^{13}C NMR δ 21.7, 28.7, 32.0, 36.0, 47.0, 47.5, 123.7, 127.8, 129.9, 133.3, 143.9, 153.7, 199.0; ESI-MS obsd 294.1155, calcd 294.1158 [$(M + H)^+$, M = $C_{15}H_{19}NO_3S$].

***N*-Tosyl-4-[2-(4-ethoxycarbonyl-3-ethylpyrrol-2-yl)-1-nitroethyl]-4-(2-oxopropyl)piperidine (8-Ts)**

Following a standard method,[38] a solution of **6** (2.73 g, 11.4 mmol) and **7-Ts** (5.00 g, 17.0 mmol) in CH_3CN (2.00 mL)

was treated with DBU (5.19 g, 34.1 mmol). The reaction mixture was stirred at room temperature for 24 h under argon. The reaction mixture was diluted with ethyl acetate, washed with a cold saturated aqueous solution of NH_4Cl, dried (Na_2SO_4), and concentrated. Column chromatography [silica, ethyl acetate–hexanes (2 : 3)] afforded a pale brown solid (4.90 g, 81%): mp 63–67 °C; ^{1}H NMR δ 1.08 (t, J = 7.2 Hz, 3H), 1.31 (t, J = 7.2 Hz, 3H), 1.72–1.94 (m, 2H), 2.09 (s, 3H), 2.10–2.18 (m, 2H), 2.44 (s, 3H), 2.33, 2.57 (AB, ^2J = 18.3 Hz, 2H), 2.45–2.47 (m, 4H), 2.99 (ABX, $^2J_{AB}$ = 15.3 Hz, $^3J_{BX}$ = 2.4 Hz, 1H), 3.18 (ABX, $^2J_{AB}$ = 15.3 Hz, $^3J_{AX}$ = 11.8 Hz, 1H), 3.52–3.68 (m, 2H), 4.23 (q, J = 7.2 Hz, 2H), 5.02 (ABX, $^3J_{AX}$ = 11.8 Hz, $^3J_{BX}$ = 2.4 Hz, 1H), 7.23 (d, J = 3.3 Hz, 1H), 7.35 (d, J = 7.8 Hz, 2H), 7.65 (d, J = 7.8 Hz, 2H), 8.36 (brs, 1H); ^{13}C NMR δ 14.6, 24.3, 30.1, 30.2, 32.0, 38.3, 41.6, 41.7, 42.7, 59.5, 93.6, 114.7, 122.5, 124.3, 125.3, 127.8, 130.1, 133.3, 144.2, 165.1, 206.5; ESI-MS obsd 556.2082, calcd 556.2088 [(M + Na)$^+$, M = $C_{26}H_{35}N_3O_7S$].

2*H*-Spiro[8-carboethoxy-7-ethyl-1-methyldipyrrin-3,4′-*N*-tosylpiperidine] (9-Ts Me)

Following a standard method,[29] in a first flask, a solution of **8-Ts** (4.45 g, 8.34 mmol) in freshly distilled THF (27 mL), was treated with NaOMe (2.25 g, 41.7 mmol) under argon at 0 °C. The mixture was stirred and degassed by bubbling argon through the solution for 45 min. In a second flask, $TiCl_3$ (33.5 mL, 20 wt% in 3% HCl solution, 53.1 mmol), THF (80 mL), NH_4OAc (33.6 g, 436 mmol), and deionized water (8.3 mL, degassed with argon for 30 min) were combined under argon, and the mixture was degassed with argon for 45 min at room temperature. Then, the first flask mixture was transferred *via* cannula to the second flask (buffered $TiCl_3$ solution). The resulting reaction mixture was stirred at room temperature for 16 h under argon. The reaction mixture was then diluted with ethyl acetate and washed with a saturated aqueous solution of $NaHCO_3$. The organic layer was washed with brine, dried (Na_2SO_4), and concentrated. Column chromatography [silica, ethyl acetate–hexanes (1 : 3)] afforded a pale yellow solid (520 mg, 13%): mp 196–198 °C; ^{1}H NMR δ 1.15 (t, J = 7.2 Hz, 3H), 1.34 (t, J = 7.2 Hz, 3H), 1.52 (dt, J = 13.8 Hz and 1.2 Hz, 2H), 1.87 (dt, J = 12.6 Hz and 3.9 Hz, 2H), 2.15 (s, 3H), 2.30–2.41 (m, 4H), 2.46 (s, 3H), 2.77 (q, J = 7.5 Hz, 2H), 3.83 (d, J = 12.3 Hz, 2H), 4.26 (q, J = 7.2 Hz, 2H), 5.70 (s, 1H), 7.35 (d, J = 8.2 Hz, 2H), 7.39 (d, J = 3.0 Hz, 1H), 7.68 (d, J = 8.2 Hz, 2H), 11.00 (brs, 1H); ^{13}C NMR δ 14.7, 16.6, 18.1, 20.8, 21.8, 36.9, 43.8, 43.9, 48.5, 59.4, 103.2, 114.3, 124.9, 126.1, 127.9, 128.1, 130.0, 133.7, 143.9, 158.9, 165.6, 176.1; ESI-MS obsd 484.2261, calcd 484.2265; [(M + H)$^+$, M = $C_{26}H_{33}N_3O_4S$]; λ_{abs} (toluene) 334 nm. During the column chromatography, a more polar component eluted after the title compound, was identified as an isomer of **7-Ts**, namely 1-(*N*-tosyl-1,2,3,6-tetrahydropyridin-4-yl)propan-2-one (**7′-Ts**), and was obtained in sizable quantity (294 mg, 12%): mp 78–80 °C; ^{1}H NMR δ 2.10 (s, 3H), 2.12–2.38 (m, 2H), 2.43 (s, 3H), 3.07 (s, 2H), 3.17–3.21 (m, 2H), 3.59–3.61 (m, 2H), 5.43–5.49 (m, 1H), 7.15 (d, J = 8.1 Hz, 2H), 7.66 (d, J = 8.1 Hz, 2H); ^{13}C NMR δ 21.7, 28.7, 29.6, 42.9, 45.0, 51.6, 121.4, 127.9, 129.8, 130.7, 133.3, 143.8, 206.3; ESI-MS obsd 294.1153, calcd 294.1158 [(M + H)$^+$, M = $C_{15}H_{19}NO_3S$].

2*H*-Spiro[8-carboethoxy-7-ethyl-1-(1,1-dimethoxymethyl)dipyrrin-3,4′-*N*-tosylpiperidine] (9-Ts-CH(OMe)$_2$)

A solution of **9-Ts-Me** (398 mg, 0.82 mmol) in 1,4-dioxane (16 mL) was treated with SeO_2 (273 mg, 2.46 mmol) under argon and stirred at room temperature. The progress of the reaction was monitored by UV-Visible spectroscopy. After 2 h, the reaction mixture was diluted with ethyl acetate, washed with a saturated aqueous solution of $NaHCO_3$, dried (Na_2SO_4), and concentrated. The crude product was used in the next step without further purification. The crude **9-Ts-CHO** [λ_{abs} (toluene) 457 nm] was dissolved in trimethyl orthoformate (7.0 mL), and TsOH·H_2O (46.8 mg, 0.246 mmol) was added at room temperature under argon. The progress of the reaction was monitored by UV-Visible spectroscopy. After 1 h, the reaction mixture was diluted with ethyl acetate, washed with water, dried (Na_2SO_4), and concentrated. Column chromatography [silica, ethyl acetate–hexanes (3 : 1)] afforded a yellow solid (187 mg, 42%): mp 80–82 °C; ^{1}H NMR δ 1.16 (t, J = 7.2 Hz, 3H), 1.34 (t, J = 7.2 Hz, 3H), 1.53 (d, J = 13.8 Hz, 2H), 1.89 (d, J = 3.9 Hz and 12.9 Hz, 2H), 2.20–2.36 (m, 2H), 2.44 (s, 2H), 2.47 (s, 3H), 2.79 (q, J = 7.2 Hz, 2H), 3.41 (s, 6H), 3.83 (d, J = 12.0 Hz, 2H), 4.27 (q, J = 7.2 Hz, 2H), 4.95 (s, 1H), 5.89 (s, 1H), 7.34 (d, J = 8.4 Hz, 2H), 7.42 (d, J = 3.3 Hz, 1H), 7.65 (d, J = 8.4 Hz, 2H), 10.78 (brs, 1H); ^{13}C NMR δ 14.6, 16.6, 18.1, 21.7, 36.9, 42.5, 42.8, 43.8, 55.2, 59.5, 103.0, 106.3, 114.5, 125.6, 127.4, 127.7, 127.8, 130.0, 133.0, 144.0, 157.7, 165.4, 173.8; ESI-MS obsd 544.2468, calcd 544.2476 [(M + H)$^+$, M = $C_{28}H_{37}N_3O_6S$]; λ_{abs} (toluene) 348 nm.

Dispiro[3,13-dicarboethoxy-2,12-diethyl-5-methoxybacteriochlorin-8,4′:18,4′′-bis(*N*-tosylpiperidine)] (MeOBCpipTs)

Following a standard method,[29] a solution of **9-Ts-CH(OMe)$_2$** (0.185 g, 0.340 mmol) in anhydrous CH_2Cl_2 (19.2 mL) was treated with 2,6-DTBP (1.52 mL, 6.80 mmol) and then with TMSOTf (0.31 mL, 1.70 mmol). The resulting reaction mixture was stirred at room temperature for 16 h. The reaction mixture was diluted with CH_2Cl_2, washed with a saturated aqueous solution of $NaHCO_3$, dried (Na_2SO_4), and concentrated. Column chromatography [silica, CH_2Cl_2–ethyl acetate (9 : 1)] afforded a purple solid (11 mg, 6.5%). During the chromatography polar oxidized products were observed (*vide infra*). Data for the title compound: ^{1}H NMR δ −2.08 (brs, 1H), −1.83 (brs, 1H), 1.56–1.78 (m, 12H), 2.08–2.19 (m, 4H), 2.58 (s, 3H), 2.59 (s, 3H), 2.76–2.96 (m, 8H), 3.80 (q, J = 7.8 Hz, 2H), 4.06–4.26 (m, 13H), 4.74 (q, J = 7.2 Hz, 4H), 7.49 (dd, J = 2.1 Hz and 8.1 Hz, 4H), 7.83 (dd, J = 2.1 Hz and 8.1 Hz, 4H), 8.52 (s, 1H), 8.64 (s, 1H), 9.55 (s, 1H); MALDI-MS obsd 990.24, ESI-MS obsd 991.4060, calcd 991.4092 [(M + H)$^+$, M = $C_{53}H_{62}N_6O_9S_2$]; λ_{abs} (CH_2Cl_2) 356, 379, 519, 735 nm. The ^{13}C NMR spectrum for this compound was not obtained owing to limited solubility. Data for one polar, oxidized product (provisionally assigned as **7-hydroxy-MeOBCpipTs** or **17-hydroxy-MeOBCpipTs**): MALDI-MS obsd 1006.92; calcd 1006.39 [M$^+$, M = $C_{53}H_{62}N_6O_{10}S_2$]; λ_{abs} (CH_2Cl_2) 359, 370, 379, 519, 725 nm. Data for a second polar,

oxidized product (provisionally assigned as a **7,17-dihydroxy-MeOBCpipTs** with unknown stereochemistry): MALDI-MS obsd 1023.31; calcd 1022.39 [M^+, M = $C_{53}H_{62}N_6O_{11}S_2$]; λ_{abs} (CH_2Cl_2) 359, 374, 379, 520, 714 nm.

1-(*N-tert*-Butoxycarbonylpiperidin-4-ylidene)propan-2-one (7-Boc)

A solution of diethyl 2-oxopropylphosphonate (25.3 g, 0.130 mol) and KOH (6.2 g, 0.11 mol) in ethanol (120 mL) at 5 °C was treated with **4-Boc** (20 g, 0.10 mol) and stirred at room temperature. After 3 days, the mixture was concentrated to dryness. The residue was triturated several times with diethyl ether at room temperature. The resulting ether solution was dried (Na_2SO_4) and concentrated. Column chromatography [silica, ethyl acetate–hexanes (2 : 3)] afforded a white solid (19.5 g, 81%): mp 70–72 °C; ^{1}H NMR δ 1.47 (s, 9H), 2.19 (s, 3H), 2.25 (t, J = 5.7 Hz, 2H), 2.90 (t, J = 5.7 Hz, 2H), 3.45 (t, J = 6.0 Hz, 2H), 3.51 (t, J = 6.0 Hz, 2H), 6.09 (s, 1H); ^{13}C NMR δ 28.3, 29.5, 31.9, 36.3, 44.4 (br), 79.8, 123.0, 155.0, 156.1, 198.9; ESI-MS obsd 262.1405; calcd 262.1414 [$(M + Na)^+$, M = $C_{13}H_{21}NO_3$]. The aforementioned data are in agreement with those for the same compound obtained *via* an independent route.[58]

N-tert-Butoxycarbonyl-4-[2-(4-ethoxycarbonyl-3-ethylpyrrol-2-yl)-1-nitroethyl]-4-(2-oxopropyl)piperidine (8-Boc)

Following a standard method,[38] solution of **2** (14.9 g, 62.0 mmol) and **7-Boc** (22.3 g, 93.0 mmol) in CH_3CN (9.5 mL) was treated with DBU (28.3 g, 186 mmol), and the reaction mixture was stirred at room temperature for 24 h under argon. The mixture was diluted with ethyl acetate, washed with a saturated aqueous solution of NH_4Cl, dried (Na_2SO_4), and concentrated. Column chromatography [silica, ethyl acetate–hexanes (2 : 3)] afforded a pale brown solid (20.5 g, 69%); mp 62–64 °C; ^{1}H NMR δ 1.14 (t, J = 7.2 Hz, 3H), 1.31 (t, J = 6.9 Hz, 3H), 1.46 (s, 9H), 1.58–1.76 (m, 3H), 1.92–2.09 (m, 1H), 2.19 (s, 3H), 2.59, 2.82 (AB, $^2J_{AB}$ = 18.3 Hz, 2H), 2.50–2.74 (m, 2H), 2.89–3.04 (m, 2H), 3.05 (ABX, $^2J_{AB}$ = 15.6 Hz, $^3J_{BX}$ = 2.4 Hz, 1H), 3.23 (ABX, $^2J_{AB}$ = 15.6 Hz, $^3J_{AX}$ = 11.4 Hz, 1H), 3.84–4.12 (brs, 2H), 4.24 (q, J = 7.2 Hz, 2H), 5.16 (ABX, $^3J_{AX}$ = 11.4 Hz, $^3J_{BX}$ = 2.4 Hz, 1H), 7.24 (d, J = 3.3 Hz, 1H), 8.54 (brs, 1H); ^{13}C NMR δ 14.6, 16.2, 18.2, 24.3, 28.6, 30.4, 32.0, 38.8, 39.0 (broad), 42.8, 59.5, 80.3, 94.0, 114.7, 122.7, 122.7, 124.3, 125.3, 154.9, 165.2, 206.9; ESI-MS obsd 502.2527, calcd 502.2524 [$(M + Na)^+$, M = $C_{24}H_{37}N_3O_7$].

2*H*-Spiro[8-carboethoxy-7-ethyl-1-methyldipyrrin-3,4′-(*N-tert*-butoxycarbonylpiperidine] (9-Boc-Me)

Following a standard method,[29] in a first flask, a solution of **8-Boc** (4.50 g, 9.38 mmol) in freshly distilled THF (30 mL) was treated with NaOMe (2.53 g, 46.9 mmol) under argon at 0 °C. The mixture was stirred and degassed by bubbling argon through the solution for 45 min. In a second flask, $TiCl_3$ (37.8 mL, 20 wt% in 3% HCl solution, 59.8 mmol), THF (90 mL), NH_4OAc (37.8 g, 490 mmol), and deionized water (9.4 mL, degassed with argon for 30 min) were combined under argon, and the mixture was degassed with argon for 45 min at room temperature. The first flask mixture was transferred *via* cannula to the second flask (buffered $TiCl_3$ solution), and the resulting reaction mixture was stirred at room temperature for 16 h under argon. Then the mixture was diluted with ethyl acetate and washed with a saturated aqueous solution of $NaHCO_3$. The organic layer was separated, dried (Na_2SO_4), and concentrated. Column chromatography [silica, ethyl acetate–hexanes (1 : 3)] afforded a colorless solid (510 mg, 13%): mp 64–66 °C; ^{1}H NMR δ 1.14 (t, J = 7.5 Hz, 3H), 1.33 (t, J = 7.2 Hz, 3H), 1.40–1.52 (m, 11H), 1.62–1.76 (m, 2H), 2.23 (s, 3H), 2.58 (s, 2H), 2.65–2.84 (m, 4H), 4.14 (d, J = 12.0 Hz, 2H), 4.26 (q, J = 7.2 Hz, 2H), 5.72 (s, 1H), 7.39 (d, J = 3.3 Hz, 1H), 11.09 (brs, 1H); ^{13}C NMR δ 14.6, 16.5, 18.1, 20.8, 28.6, 37.3, 41.4, 44.7, 48.2, 59.4, 80.0, 103.0, 114.2, 124.8, 125.8, 128.3, 155.0, 159.8, 165.7, 176.6; ESI-MS obsd 430.2705, calcd 430.2700 [$(M + H)^+$, M = $C_{24}H_{35}N_3O_4$].

A refined procedure is as follows. In a first flask, samples of NH_4OAc (33.8 g, 439 mmol), freshly distilled THF (81 mL), $TiCl_3$ (33.8 mL, 20 wt% in 3% HCl solution, 53.6 mmol), and 15 mL of deionized water (degassed with argon for 30 min) were combined under argon, and the mixture was degassed with argon for 40 min at room temperature. In a second flask, a solution of **8-Boc** (4.03 g, 8.40 mmol) in freshly distilled THF (26 mL) at 0 °C was treated with NaOMe (1.13 g, 21.0 mmol) under argon. The mixture was bubbled with argon and stirred at 0 °C for 3 min. Then, the solution was transferred *via* cannula to the first flask (buffered $TiCl_3$ solution). The resulting reaction mixture was stirred at room temperature for 18 h under argon. Then, the reaction mixture was diluted with ethyl acetate and washed with a saturated aqueous solution of $NaHCO_3$. The organic layer was separated, dried (Na_2SO_4), and concentrated. Column chromatography [silica, ethyl acetate–hexanes (1 : 3)] afforded a pale yellow solid (1.5 g, 41%): ^{1}H NMR (400 MHz) δ 1.15 (t, J = 7.6 Hz, 3H), 1.34 (t, J = 7.2 Hz, 3H), 1.42–1.52 (m, 11H), 1.62–1.74 (m, 2H), 2.24 (s, 3H), 2.58 (s, 2H), 2.68–2.84 (m, 4H), 4.04–4.22 (br, 2H), 4.27 (q, J = 7.2 Hz, 2H), 5.74 (s, 1H), 7.41 (d, J = 2.8 Hz, 1H), 11.10 (brs, 1H); ^{13}C NMR δ 14.6, 16.5, 18.1, 20.8, 28.6, 37.3, 41.2 (br), 44.7, 48.2, 59.4, 80.0, 102.8, 114.2, 124.8, 125.8, 128.3, 155.0, 159.8, 165.7, 176.7; ESI-MS obsd 430.2701; calcd 430.2700 [$(M + H)^+$, M = $C_{24}H_{35}N_3O_4$]; λ_{abs} (toluene) 334 nm; λ_{abs} (diethyl ether) 331 nm.

2*H*-Spiro[8-carboethoxy-7-ethyl-1-(1,1-dimethoxymethyl)dipyrrin-3,4′-*N-tert*-butoxycarbonylpiperidine] (9-Boc-CH(OMe)$_2$)

A solution of **9-Boc-Me** (500 mg, 1.16 mmol) in 1,4-dioxane (23 mL) was treated with SeO_2 (387 mg, 3.49 mmol) under argon. The reaction mixture was stirred at room temperature, and the progress of the reaction was monitored by UV-Visible spectroscopy. After 1 h, the reaction mixture was diluted with ethyl acetate, washed with water, dried (Na_2SO_4), and concentrated; the crude product was used in the next step without further purification. The crude **9-Boc-CHO** [λ_{abs} (toluene) 453 nm; λ_{abs} (diethyl ether) 448 nm] was dissolved in trimethyl orthoformate (10 mL), and TsOH·H_2O (66.0 mg, 0.35 mmol) was added at room temperature under argon. The progress of the reaction was monitored by UV-Visible spectroscopy. After 1 h, the reaction mixture was diluted with ethyl acetate and washed

with a saturated aqueous solution of $NaHCO_3$. The organic layer was separated, dried (Na_2SO_4), and concentrated. Column chromatography [silica, ethyl acetate–hexanes (3 : 1)] afforded a yellow oil (252 mg, 44%): ^{1}H NMR δ 1.16 (t, J = 7.6 Hz, 3H), 1.34 (t, J = 7.2 Hz, 3H), 1.43–1.48 (m, 2H), 1.49 (s, 9H), 1.65–1.75 (m, 2H), 2.70 (s, 2H), 2.74–2.86 (m, 4H), 3.46 (s, 6H), 4.15 (brs, 2H), 4.27 (q, J = 7.2 Hz, 2H), 5.02 (s, 1H), 5.88 (s, 1H), 7.43 (d, J = 3.2 Hz, 1H), 10.87 (brs, 1H); ^{13}C NMR δ 14.7, 16.6, 18.2, 28.7, 37.4, 41.1, 42.6, 43.7, 55.1, 59.5, 80.0, 103.0, 105.9, 114.5, 125.5, 127.1, 127.9, 155.0, 158.7, 165.5, 174.4; ESI-MS obsd 490.2909; calcd 490.2912 [(M + H)$^+$, M = $C_{26}H_{39}N_3O_6$]; λ_{abs} (toluene) 344 nm; λ_{abs} (diethyl ether) 344 nm. The same procedure at 2.8-times the scale afforded the title compound (630 mg) in 39% yield.

Dispiro[3,13-dicarboethoxy-2,12-diethylbacteriochlorin-8,4′:18,4′′-bis(*N*,*N*-dimethylpiperidinium iodide)] (BCpipMe$_2$I)

A solution of **9-Boc-CH(OMe)$_2$** (0.10 g, 0.20 mmol, 18 mM) in CH_3CN (11.5 mL) was treated with $BF_3{\cdot}OEt_2$ (0.20 mL, 1.6 mmol, 140 mM) dropwise at room temperature, and the reaction mixture was stirred at room temperature under argon for 16 h. The reaction mixture was then diluted with ethyl acetate and washed with a saturated aqueous solution of $NaHCO_3$. The organic layer was dried (Na_2SO_4) and concentrated to afford the crude bacteriochlorin **BCpip** with the following characterization data: MALDI-MS obsd 651.77; ESI-MS obsd 653.3798, calcd 653.3810 [(M + H)$^+$, M = $C_{38}H_{48}N_6O_4$]; λ_{abs} (CH_2Cl_2) 353, 381, 517, 750 nm. A 25 mg sample of the crude bacteriochlorin **BCpip** was carried forward. Thus, the 25 mg of crude **BCpip** in $CHCl_3$ (3 mL) was treated with K_2CO_3 (26 mg, 0.19 mmol) followed by MeI (0.048 mL, 0.76 mmol), and the reaction mixture was stirred at room temperature for 16 h. The excess MeI and $CHCl_3$ were removed under reduced pressure at ambient temperature. Diethyl ether (20 mL) was added to the crude product. The mixture was sonicated for 2 min and centrifuged. The supernatant was removed to afford a solid (25 mg, 34% from the two steps of condensation and alkylation but not all crude was used in the second step): MALDI-MS obsd 695.10 (M-15); ESI-MS obsd 355.2259, calcd 355.2254 [M^{2+}, M = $C_{42}H_{58}N_6O_4$]; λ_{abs} (H_2O) 352, 378, 518, 747 nm.

Dispiro[3,13-dicarboethoxy-2,12-diethyl-5-methoxybacteriochlorin-8,4′:18,4′′-bis(*N*-methylpiperidine)] (MeOBCpipMe)

Following a standard method,[29] a solution of **9-Boc-CH(OMe)$_2$** (430 mg, 0.878 mmol, 18 mM) in anhydrous CH_2Cl_2 (49 mL) was first treated with 2,6-DTBP (3.94 mL, 17.5 mmol, 360 mM) and second with TMSOTf (0.79 mL, 4.38 mmol, 90 mM). The reaction mixture was stirred at room temperature for 16 h. The solution was diluted with ethyl acetate and washed with a saturated aqueous solution of $NaHCO_3$. The organic layer was separated, dried (Na_2SO_4), and concentrated to afford **MeOBCpip** in crude form with the following characterization data: LD-MS obsd 684.07, ESI-MS obsd 683.3891; calcd 683.3915 [(M + H)$^+$, M = $C_{39}H_{50}N_6O_5$]; λ_{abs} (CH_2Cl_2) 356, 379, 520, 738 nm]. The crude product **MeOBCpip** (720 mg, far in excess of the theoretical yield due to the presence of 2,6-DTBP and other species) in its entirety was used directly in the next step (with a slightly modified procedure[59]). Thus, a solution of all of the crude **MeOBCpip** in CF_3CH_2OH (45 mL) was treated with paraformaldehyde (132 mg, 4.39 mmol) at 78 °C. After 10 min, the reaction mixture was treated with $NaBH_4$ (66.0 mg, 1.76 mmol) and stirred at 78 °C for 2 h. The mixture was diluted with ethyl acetate, washed with deionized water, dried (Na_2SO_4), and concentrated. The residue was chromatographed [silica, ethyl acetate–triethylamine–MeOH (8 : 1 : 1)] to afford a purple solid (140.0 mg, 45% for the two steps): ^{1}H NMR δ −1.98 (brs, 1H), −1.71 (brs, 1H), 1.58–1.79 (m, 12H), 2.06–2.2 (m, 4H), 2.64 (s, 6H), 2.65–3.01 (m, 8H), 3.30 (brs, 4H), 3.79 (q, J = 7.2 Hz, 2H), 4.12 (q, J = 7.2 Hz, 2H), 4.23 (s, 3H), 4.39 (s, 2H), 4.45 (s, 2H), 4.77 (q, J = 7.2 Hz, 4H), 8.67 (s, 1H), 8.79 (s, 1H), 9.63 (s, 1H); ^{13}C NMR δ 14.77, 14.83, 17.8, 17.9, 20.2, 20.8, 39.6, 39.7, 43.2, 46.9, 47.2, 48.5, 48.8, 53.2, 53.4, 61.0, 62.0, 64.7, 94.5, 96.0, 97.7, 118.7, 124.5, 128.0, 132.3, 134.0, 134.9, 135.3, 136.1, 142.3, 155.9, 160.8, 166.6, 167.0, 168.9, 170.1; MALDI-MS obsd 710.59; ESI-MS obsd 711.4225; calcd 711.4228 [(M + H)$^+$, M = $C_{41}H_{54}N_6O_5$]; λ_{abs} (CH_2Cl_2) 356, 379, 520, 738 nm.

Dispiro[3,13-dicarboethoxy-2,12-diethyl-5-methoxybacteriochlorin-8,4′:18,4′′-bis(*N*,*N*-dimethylpiperidinium iodide)] (MeOBCpipMe$_2$I)

A solution of **MeOBCpipMe** (4.3 mg, 0.0060 mmol) in $CHCl_3$ (0.5 mL, 12 mM) was treated with MeI (30 μL, 0.24 mmol) and stirred at room temperature for 24 h. The excess MeI and $CHCl_3$ were removed under reduced pressure at room temperature. Diethyl ether (6 mL) was added to the crude product. The mixture was sonicated for 2 min and centrifuged. The supernatant was removed, affording the desired product as a solid (4.8 mg, 82%): MALDI-MS obsd 725.50 (M–15); ESI-MS obsd 370.2305; calcd 370.2307 [M^{2+}, M = $C_{43}H_{60}N_6O_5$]; λ_{abs} (H_2O) 353, 519, 732 nm.

Dispiro[3,13-dicarboethoxy-2,12-diethyl-5-methoxybacteriochlorin-8,4′:18,4′′-bis(*N*-acetylpiperidine)] (MeOBCpipAc)

Following a standard method,[29] a solution of **9-Boc-CH(OMe)$_2$** (400 mg, 0.816 mmol, 18 mM) was condensed as described above to afford the crude bacteriochlorin **MeOBCpip** (250 mg). A sample of 68.2 mg of the crude bacteriochlorin (0.273-fold of the total 250 mg) was carried forward. Thus, a solution of crude bacteriochlorin **MeOBCpip** (68.2 mg) in CH_2Cl_2 (10 mL, 10 mM) was treated with acetyl chloride (177 μL, 0.25 mmol) and stirred at room temperature for 2 h. The reaction mixture was diluted with CH_2Cl_2 and washed with 2% HCl and water. The organic layer was dried (Na_2SO_4) and concentrated. The residue was chromatographed [silica, ethyl acetate–triethylamine–MeOH (8 : 2 : 1)] to afford a green solid (40 mg, 47% on the basis of the split quantity of crude bacteriochlorin taken forward for acylation): ^{1}H NMR δ −1.99 (brs, 1H), −1.74 (brs, 1H), 1.63 (t, J = 6.8 Hz, 3H), 1.68–1.78 (m, 9H), 2.02–2.24 (m, 4H), 2.33 (s, 6H), 2.45–2.75 (m, 4H), 3.10–3.28 (m, 2H), 3.68–3.89 (m, 4H), 4.06–4.20 (m, 4H), 4.24 (s, 3H), 4.41–4.59 (m, 4H), 4.78 (q, J = 7.2 Hz, 4H), 5.02–5.14 (m, 2H), 8.49 (s, 1H), 8.61 (s, 1H), 9.68 (s, 1H); ^{13}C NMR δ 14.8, 14.8, 17.8, 18.0, 20.2, 20.9, 22.0, 38.5, 38.6, 39.5, 42.5, 46.5, 49.5, 49.8, 61.1, 62.1, 64.8, 94.3, 95.7, 98.0, 119.1, 124.8, 128.0, 132.3, 134.0, 135.1, 135.4, 136.3, 142.6,

155.3, 160.1, 165.7, 166.5, 168.7, 168.5, 169.5; MALDI-MS obsd 766.06; ESI-MS obsd 767.4127; calcd 767.4114 [$(M + H)^+$, M = $C_{43}H_{54}N_6O_7$]; λ_{abs} (CH_2Cl_2) 356, 379, 519, 736 nm.

Dispiro[3,13-dicarboethoxy-2,12-diethyl-5-methoxybacteriochlorin-8,4′:18,4′′-bis(*N*-butylsulfonylpiperidine)] (MeOBCpipSO$_2$Bu)

A sample of 121 mg of the crude bacteriochlorin **MeOBCpip** (0.484-fold of the total 250 mg) obtained as described in the prep of **MeOBCpipAc** was carried forward for the sulfonylation. Thus, a solution of crude bacteriochlorin **MeOBCpip** (121 mg) in CH_2Cl_2 (17 mL, 10 mM) containing triethylamine (1 mL) was treated with butylsulfonyl chloride (470 μL, 0.358 mmol) and stirred at room temperature for 2 h. The reaction mixture was diluted with CH_2Cl_2 and washed with a saturated aqueous solution of $NaHCO_3$ and water. The organic layer was dried (Na_2SO_4) and concentrated. The residue was chromatographed [silica, ethyl acetate–hexanes (3 : 7)] to afford a green solid (70 mg, 38% on the basis of the split quantity of crude bacteriochlorin taken forward for sulfonylation): ^{1}H NMR δ −2.03 (brs, 1H), −1.77 (brs, 1H), 1.07 (t, J = 7.2 Hz, 6H), 1.52–1.79 (m, 16H), 1.92–2.04 (m, 4H), 2.12–2.20 (m, 4H), 2.65–2.82 (m, 4H), 3.06–3.18 (m, 4H), 3.28–3.49 (m, 4H), 3.82 (q, J = 7.6 Hz, 2H), 4.02–4.20 (m, 6H), 4.24 (s, 3H), 4.41 (s, 2H), 4.46 (s, 2H), 4.78 (q, J = 7.6 Hz, 4H), 8.54 (s, 1H), 8.66 (s, 1H), 9.67 (s, 1H) ^{13}C NMR δ 14.8, 14.8, 17.8, 18.0, 20.2, 20.9, 22.0, 38.5, 38.6, 39.5, 42.5, 46.5, 49.5, 49.8, 61.1, 62.1, 64.8, 94.3, 95.7, 98.0, 119.1, 124.8, 128.0, 132.3, 134.0, 135.1, 135.40, 136.3, 142.6, 155.3, 160.1, 165.7, 166.5, 168.7, 168.5, 169.5; MALDI-MS obsd 922.22; ESI-MS obsd 923.4380; calcd 923.4405 [$(M + H)^+$, M = $C_{47}H_{66}N_6O_9S_2$]; λ_{abs} (CH_2Cl_2) 357, 379, 519, 735 nm.

Photophysical measurements

Static absorption measurements employed a Varian Cary 50 or 100 or Shimadzu UV-1800 spectrometer. Static fluorescence measurements employed a Spex Fluorolog Tau 2 or PTI Quantamaster 40 spectrofluorometer. Fluorescence lifetimes were obtained *via* decay measurements using a Photon Technology International LaserStrobe TM-3, composed of a GL-3300 nitrogen laser with a GL-302 dye laser unit and time-correlated-single-photon-counting detection. The apparatus has an approximately Gaussian instrument response function with a full-width-at-half-maximum of ∼1 ns. Excitation pulses were provided by the nitrogen-pumped dye laser (350–650 nm). Static emission measurements employed 0.2 nm data intervals and typical monochromator bandwidths of 2–4 nm using a setup containing a Hamamatsu R928 photomultiplier tube. Emission spectra were corrected for detection-system spectral response. The standards used for fluorescence yield determinations[48] were (1) free base *meso*-tetraphenylporphyrin (**FbTPP**) in nondegassed toluene, for which Φ_f = 0.070 was established with respect to the zinc chelate **ZnTPP** in nondegassed toluene (Φ_f = 0.030),[65] consistent with prior results on **FbTPP**,[66] (2) 8,8,18,18-tetramethylbacteriochlorin[48] in argon-purged toluene, for which Φ_f = 0.14 was established with respect to **FbTPP** and chlorophyll *a* (**Chl *a***) in deoxygenated benzene[67] or toluene[68] (both with Φ_f = 0.325). Measurements of fluorescence spectra, fluorescence excitation spectra, fluorescence quantum yields, and fluorescence lifetimes employed samples having an absorbance $A \leq 0.1$ at the excitation wavelength(s).

Time-resolved pump–probe absorption experiments were performed to complement excited-state lifetime measurements by fluorescence and to determine yields of intersystem crossing (*e.g.*, triplet) yields. These measurements were carried out using a Helios femtosecond transient absorption spectrometer (Ultrafast Systems) coupled to a femtosecond laser system (Newport/Spectra-Physics). The one-box Solstice amplified ultrafast laser system produces 800 nm pulses (∼3.5 mJ, ∼0.1 ps) at 1 kHz. The output beam is split into two and used to generate (i) the pump beam (90%) in a Topas-C optical parametric amplifier (Light Conversion, Lithuania) and (ii) probe pulses (10%) for the Helios transient-absorption spectrometer. The pump (excitation) pulses pass through a depolarizer to provide isotropic excitation of the sample and avoid pump–probe polarization effects. Individual ΔA spectra are acquired using excitation light chopped at 0.5 kHz (to provide alternate accumulations of the probe light with and without excitation) and averaged over 1–5 s (typically 2 s). Final ΔA spectra represent the average of 1000 such individual spectra. The excitation pulses (typically of energy 0.5 μJ per pulse) were adjusted to have a spot diameter of 1 mm.

The intersystem crossing (triplet) yield values were obtained using a transient-absorption technique in which the extent of bleaching of the ground-state Q_x and Q_y bands due to the lowest singlet excited state was measured immediately following an 0.1 ps flash (in the Q_x or Q_y bands) and compared with that due to the lowest triplet excited state at the asymptote of the singlet excited-state decay. For the Q_y region, the contribution of stimulated emission was taken into account. For both states and spectral regions, the extent of bleaching in the presence of excited-state absorption in the transient difference spectra was determined by various methods (to encompass a reasonable range of spectral shapes) including Gaussian fitting, integrations, and linear interpolation of the excited-state absorption across the ground-state bleaching region. An average value of the triplet yields obtained by these methods is reported for each bacteriochlorin.

Acknowledgements

This research was carried out as part of the Photosynthetic Antenna Research Center (PARC), an Energy Frontier Research Center funded by the U.S. Department of Energy, Office of Science, Office of Basic Energy Sciences, under Award No. DE-SC0001035. Mass spectra were obtained at the Mass Spectrometry Laboratory for Biotechnology at North Carolina State University. Partial funding for the facility was obtained from the North Carolina Biotechnology Center and the National Science Foundation. We thank Ms Jina Whang for technical assistance.

References

1 M. Kobayashi, M. Akiyama, H. Kano and H. Kise, in *Chlorophylls and Bacteriochlorophylls: Biochemistry, Biophysics, Functions and Applications*, ed. B. Grimm, R. J. Porra,

W. Rüdiger and H. Scheer, Springer, Dordrecht, The Netherlands, 2006, pp. 79–94.
2 J. R. Stromberg, A. Marton, H. L. Kee, C. Kirmaier, J. R. Diers, C. Muthiah, M. Taniguchi, J. S. Lindsey, D. F. Bocian, G. J. Meyer and D. Holten, *J. Phys. Chem. C*, 2007, **111**, 15464–15478.
3 C. Muthiah, H. L. Kee, J. R. Diers, D. Fan, M. Ptaszek, D. F. Bocian, D. Holten and J. S. Lindsey, *Photochem. Photobiol.*, 2008, **84**, 786–801.
4 J. S. Lindsey, O. Mass and C.-Y. Chen, *New J. Chem.*, 2011, **35**, 511–516.
5 J. W. Springer, P. S. Parkes-Loach, K. R. Reddy, M. Krayer, J. Jiao, G. M. Lee, D. M. Niedzwiedzki, M. A. Harris, C. Kirmaier, D. F. Bocian, J. S. Lindsey, D. Holten and P. A. Loach, *J. Am. Chem. Soc.*, 2012, **134**, 4589–4599.
6 J. M. Sutton, O. J. Clarke, N. Fernandez and R. W. Boyle, *Bioconjugate Chem.*, 2002, **13**, 249–263.
7 Y. Chen, G. Li and R. K. Pandey, *Curr. Org. Chem.*, 2004, **8**, 1105–1134.
8 O. Mazor, A. Brandis, V. Plaks, E. Neumark, V. Rosenbach-Belkin, Y. Salomon and A. Scherz, *Photochem. Photobiol.*, 2005, **81**, 342–351.
9 M. A. Grin, A. F. Mironov and A. A. Shtil, *Anti-Cancer Agents Med. Chem.*, 2008, **8**, 683–697.
10 H. L. Kee, R. Nothdurft, C. Muthiah, J. R. Diers, D. Fan, M. Ptaszek, D. F. Bocian, J. S. Lindsey, J. P. Culver and D. Holten, *Photochem. Photobiol.*, 2008, **84**, 1061–1072.
11 P. Mroz, Y.-Y. Huang, A. Szokalska, T. Zhiyentayev, S. Janjua, A.-P. Nifli, M. E. Sherwood, C. Ruzié, K. E. Borbas, D. Fan, M. Krayer, T. Balasubramanian, E. Yang, H. L. Kee, C. Kirmaier, J. R. Diers, D. F. Bocian, D. Holten, J. S. Lindsey and M. R. Hamblin, *FASEB J.*, 2010, **24**, 3160–3170.
12 Y.-Y. Huang, P. Mroz, T. Zhiyentayev, S. K. Sharma, T. Balasubramanian, C. Ruzié, M. Krayer, D. Fan, K. E. Borbas, E. Yang, H. L. Kee, C. Kirmaier, J. R. Diers, D. F. Bocian, D. Holten, J. S. Lindsey and M. R. Hamblin, *J. Med. Chem.*, 2010, **53**, 4018–4027.
13 L. Huang, Y.-Y. Huang, P. Mroz, G. P. Tegos, T. Zhiyentayev, S. K. Sharma, Z. Lu, T. Balasubramanian, M. Krayer, C. Ruzié, E. Yang, H. L. Kee, C. Kirmaier, J. R. Diers, D. F. Bocian, D. Holten, J. S. Lindsey and M. R. Hamblin, *Antimicrob. Agents Chemother.*, 2010, **54**, 3834–3841.
14 S. Singh, A. Aggarwal, S. Thompson, J. P. C. Tomé, X. Zhu, D. Samaroo, M. Vinodu, R. Gao and C. M. Drain, *Bioconjugate Chem.*, 2010, **21**, 2136–2146.
15 L. G. Arnaut, *Inorg. Photochem.*, 2011, **63**, 187–233.
16 J. M. Dąbrowski, K. Urbanska, L. G. Arnaut, M. M. Pereira, A. R. Abreu, S. Simões and G. Stochel, *ChemMedChem*, 2011, **6**, 465–475.
17 V. M. Alexander, K. Sano, Z. Yu, T. Nakajima, P. L. Choyke, M. Ptaszek and H. Kobayashi, *Bioconjugate Chem.*, 2012, **23**, 1671–1679.
18 C. J. P. Monteiro, J. Pina, M. M. Pereira and L. G. Arnaut, *Photochem. Photobiol. Sci.*, 2012, **11**, 1233–1238.
19 H. Scheer, in *Chlorophylls and Bacteriochlorophylls: Biochemistry, Biophysics, Functions and Applications*, ed. B. Grimm, R. J. Porra, W. Rüdiger and H. Scheer, Springer, Dordrecht, The Netherlands, 2006, pp. 1–26.
20 A. M. G. Silva, A. C. Tomé, M. G. P. M. S. Neves, A. M. S. Silva and J. A. S. Cavaleiro, *J. Org. Chem.*, 2005, **70**, 2306–2314.
21 M. Galezowski and D. T. Gryko, *Curr. Org. Chem.*, 2007, **11**, 1310–1338.
22 A. C. Tomé, M. G. P. M. S. Neves and J. A. S. Cavaleiro, *J. Porphyrins Phthalocyanines*, 2009, **13**, 408–414.
23 N. A. M. Pereira, S. M. Fonseca, A. C. Serra, T. M. V. D. Pinho e Melo and H. D. Burrows, *Eur. J. Org. Chem.*, 2011, 3970–3979.
24 Z. Yu and M. Ptaszek, *Org. Lett.*, 2012, **14**, 3708–3711.
25 L. P. Samankumara, S. Wells, M. Zeller, A. M. Acuña, B. Röder and C. Brückner, *Angew. Chem., Int. Ed.*, 2012, **51**, 5757–5760.
26 C. Brückner, L. Samankumara and J. Ogikubo, in *Handbook of Porphyrin Science*, ed. K. M. Kadish, K. M. Smith and R. Guilard, World Scientific, Singapore, 2012, vol. 17, pp. 1–112.
27 H.-J. Kim and J. S. Lindsey, *J. Org. Chem.*, 2005, **70**, 5475–5486.
28 M. Taniguchi, D. L. Cramer, A. D. Bhise, H. L. Kee, D. F. Bocian, D. Holten and J. S. Lindsey, *New J. Chem.*, 2008, **32**, 947–958.
29 M. Krayer, M. Ptaszek, H.-J. Kim, K. R. Meneely, D. Fan, K. Secor and J. S. Lindsey, *J. Org. Chem.*, 2010, **75**, 1016–1039.
30 M. Krayer, E. Yang, J. R. Diers, D. F. Bocian, D. Holten and J. S. Lindsey, *New J. Chem.*, 2011, **35**, 587–601.
31 O. Mass and J. S. Lindsey, *J. Org. Chem.*, 2011, **76**, 9478–9487.
32 P. D. Harvey, in *The Porphyrin Handbook*, ed. K. M. Kadish, K. M. Smith and R. Guilard, Academic Press, San Diego, CA, 2003, vol. 18, pp. 63–250.
33 P. D. Harvey, C. Stern and R. Guilard, in *Handbook of Porphyrin Science*, ed. K. M. Kadish, K. M. Smith and R. Guilard, World Scientific Publishing Co., Singapore, 2011, vol. 11, pp. 1–179.
34 C. Ruzié, M. Krayer, T. Balasubramanian and J. S. Lindsey, *J. Org. Chem.*, 2008, **73**, 5806–5820.
35 P. Hambright, in *The Porphyrin Handbook*, ed. K. M. Kadish, K. M. Smith and R. Guilard, Academic Press, San Diego, CA, 2000, vol. 3, pp. 129–210.
36 C. Ruzié, M. Krayer and J. S. Lindsey, *Org. Lett.*, 2009, **11**, 1761–1764.
37 C.-Y. Chen, E. Sun, D. Fan, M. Taniguchi, B. E. McDowell, E. Yang, J. R. Diers, D. F. Bocian, D. Holten and J. S. Lindsey, *Inorg. Chem.*, 2012, **51**, 9443–9464.
38 K. E. Borbas, C. Ruzié and J. S. Lindsey, *Org. Lett.*, 2008, **10**, 1931–1934.
39 M. Taniguchi, H.-J. Kim, D. Ra, J. K. Schwartz, C. Kirmaier, E. Hindin, J. R. Diers, S. Prathapan, D. F. Bocian, D. Holten and J. S. Lindsey, *J. Org. Chem.*, 2002, **67**, 7329–7342.
40 F. Diederich and K. Dick, *Tetrahedron Lett.*, 1982, **23**, 3167–3170.
41 F. Diederich and K. Dick, *Angew. Chem., Int. Ed. Engl.*, 1983, **22**, 715–716.

42 F. Diederich and K. Dick, *J. Am. Chem. Soc.*, 1984, **106**, 8024–8036.
43 F. Diederich, K. Dick and D. Griebel, *Chem. Ber.*, 1985, **118**, 3588–3619.
44 S. B. Ferguson, E. M. Sanford, E. M. Seward and F. Diederich, *J. Am. Chem. Soc.*, 1991, **113**, 5410–5419.
45 B. Hinzen, P. Seiler and F. Diederich, *Helv. Chim. Acta*, 1996, **79**, 942–960.
46 E. A. Meyer, R. K. Castellano and F. Diederich, *Angew. Chem., Int. Ed.*, 2003, **42**, 1210–1250.
47 G. P. Moss, *Pure Appl. Chem.*, 1999, **71**, 531–558.
48 E. Yang, C. Kirmaier, M. Krayer, M. Taniguchi, H.-J. Kim, J. R. Diers, D. F. Bocian, J. S. Lindsey and D. Holten, *J. Phys. Chem. B*, 2011, **115**, 10801–10816.
49 A. J. Peat, P. R. Sebahar, M. Youngman, P. Y. Chong and H. Zhang, *PCT Int. Appl.*, *WO*2008154271, 2008.
50 R. W. Lang and H.-J. Hansen, *Org. Synth.*, 1984, **62**, 202–206.
51 P. A. Jacobi, S. Lanz, I. Ghosh, S. H. Leung, F. Löwer and D. Pippin, *Org. Lett.*, 2001, **3**, 831–834.
52 H.-J. Kim, D. K. Dogutan, M. Ptaszek and J. S. Lindsey, *Tetrahedron*, 2007, **63**, 37–55.
53 M. K. Basu, S. Samajdar, F. F. Becker and B. K. Banik, *Synlett*, 2002, 319–321.
54 B. Qin, X. Liu, J. Shi, K. Zheng, H. Zhao and X. Feng, *J. Org. Chem.*, 2007, **72**, 2374–2378.
55 J. Bonjoch, N. Casamitjana and J. Bosch, *Tetrahedron*, 1982, **38**, 2883–2888.
56 R. Sebesta, M. G. Pizzuti, A. J. Boersma, A. J. Minnaard and B. L. Feringa, *Chem. Commun.*, 2005, 1711–1713.
57 M. D. Kosobokov, I. D. Titanyuk and I. P. Beletskaya, *Mendeleev Commun.*, 2011, **21**, 142–143.
58 D. P. Walker, B. A. Acker, E. J. Jacobsen and D. G. Wishka, *J. Heterocycl. Chem.*, 2008, **45**, 247–257.
59 M. Tajbakhsh, R. Hosseinzadeh, H. Alinezhad, S. Ghahari, A. Heydari and S. Khaksar, *Synthesis*, 2011, 490–496.
60 N. Srinivasan, C. A. Haney, J. S. Lindsey, W. Zhang and B. T. Chait, *J. Porphyrins Phthalocyanines*, 1999, **3**, 283–291.
61 J. S. Lindsey, *Acc. Chem. Res.*, 2010, **43**, 300–311.
62 M. O. Senge, *Chem. Commun.*, 2011, **47**, 1943–1960.
63 A. Musenga, A. Schedle, U. Demelbauer, L. Kremser, M. A. Raggi and E. Kenndler, *J. Chromatogr., A*, 2004, **1034**, 221–226.
64 Z. S. Saify, H. Rasheed, N. Mushtaq, M. Nisa, S. Haider, A. Naz, K. F. Azhar and G. A. Miana, *Arch. Pharmacal Res.*, 2012, **35**, 1953–1959.
65 P. G. Seybold and M. Gouterman, *J. Mol. Spectrosc.*, 1969, **31**, 1–13.
66 A. T. Gradyushko, A. N. Sevchenko, K. N. Solovyov and M. P. Tsvirko, *Photochem. Photobiol.*, 1970, **11**, 387–400.
67 G. Weber and F. W. J. Teale, *Trans. Faraday Soc.*, 1957, **53**, 646–655.
68 O. Mass, M. Taniguchi, M. Ptaszek, J. W. Springer, K. M. Faries, J. R. Diers, D. F. Bocian, D. Holten and J. S. Lindsey, *New J. Chem.*, 2011, **35**, 76–88.